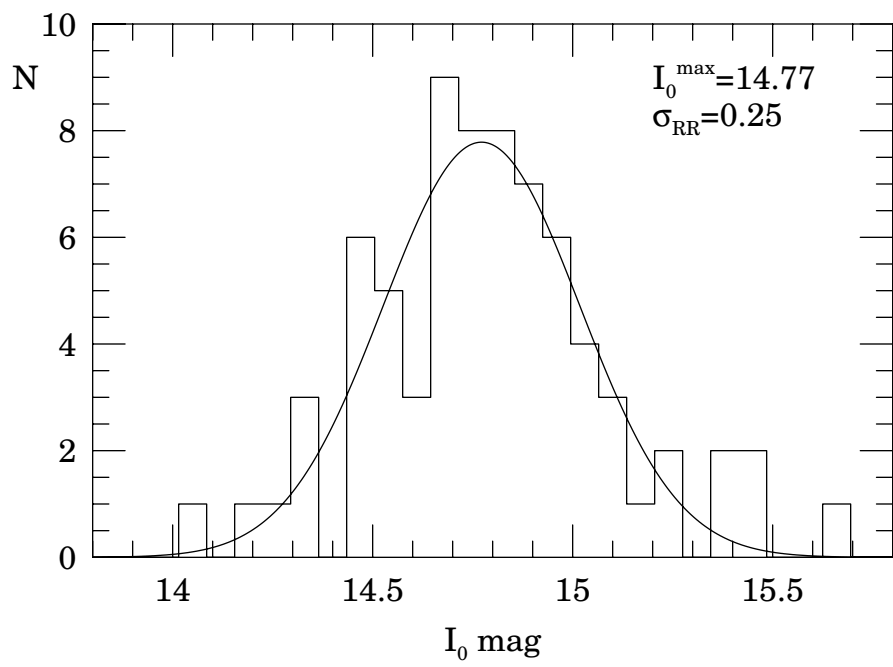
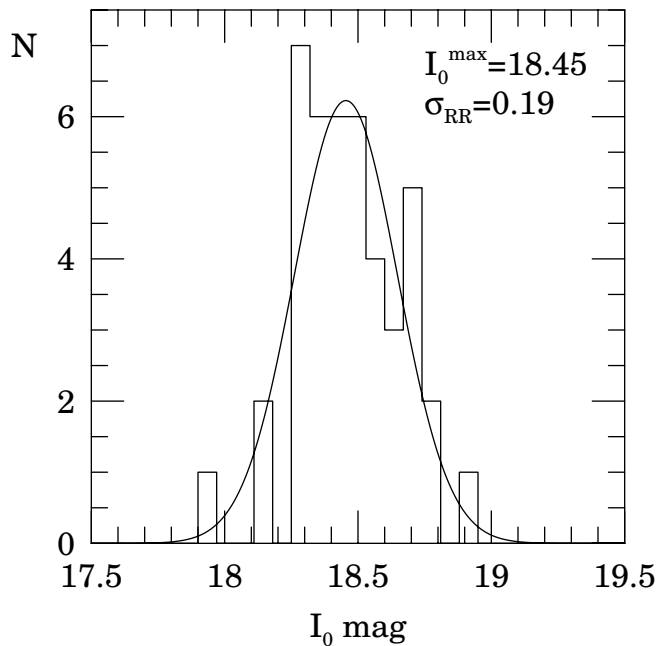


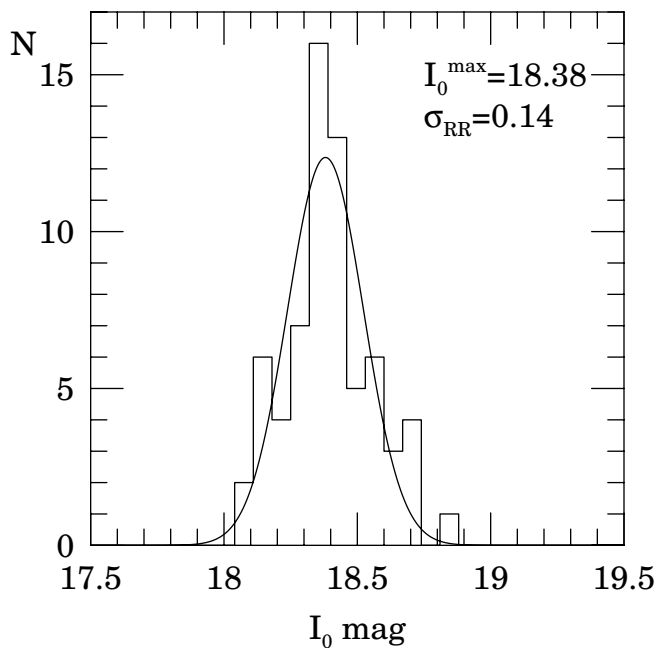
RR LYRAE - GALACTIC BULGE (BW)



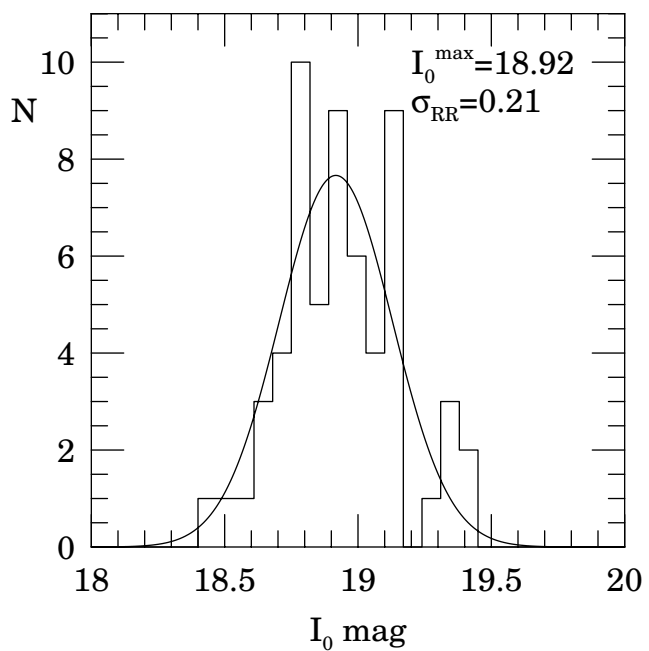
RR LYRAE - LMC_E



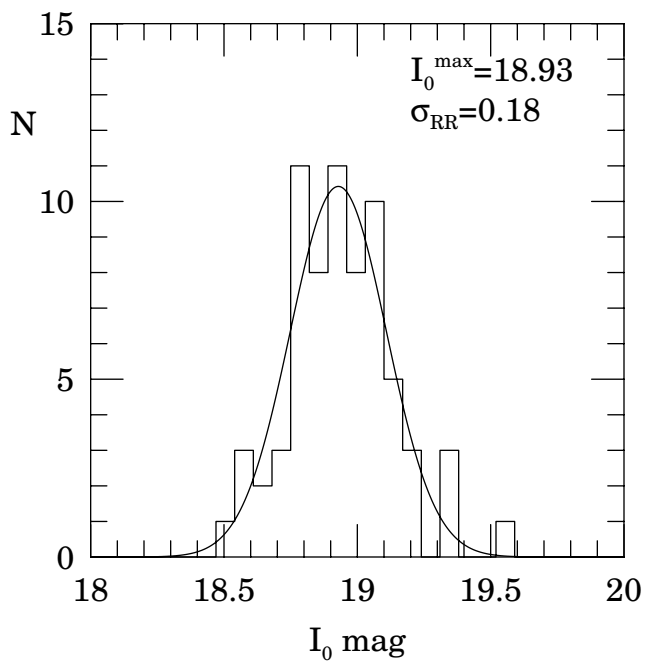
RR LYRAE - LMC_W



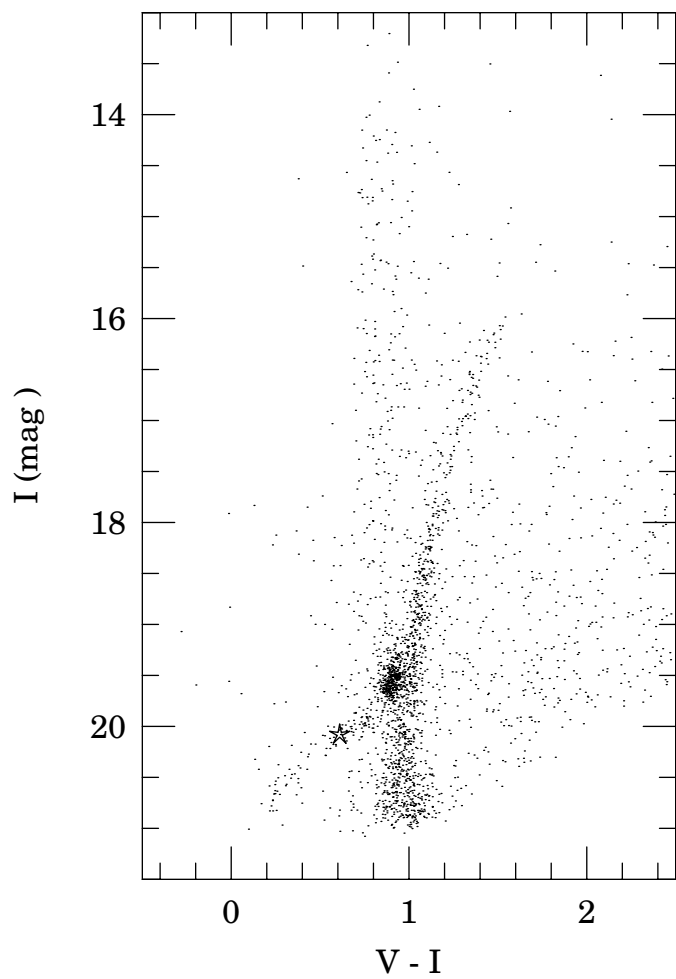
RR LYRAE - SMC_E



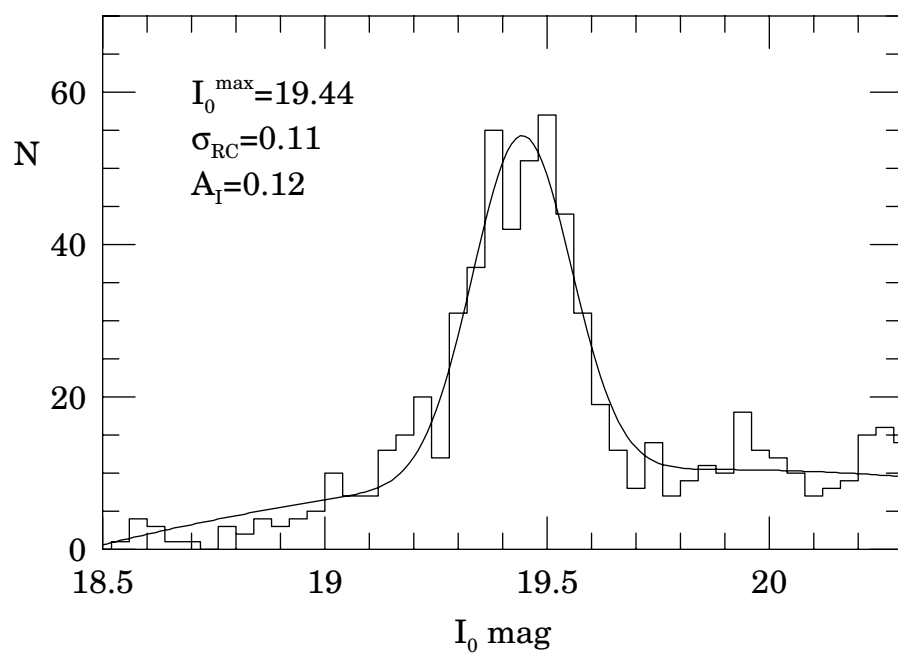
RR LYRAE - SMC_W

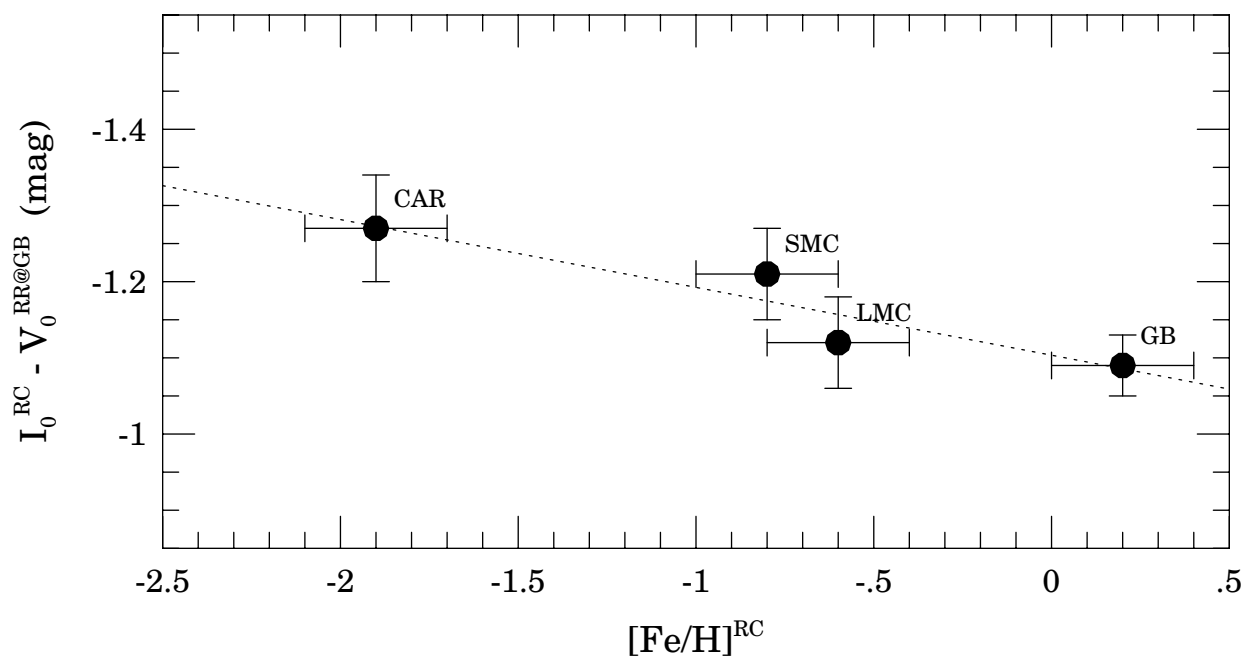


CARINA DWARF GALAXY



RED CLUMP - CARINA DWARF GALAXY





The Optical Gravitational Lensing Experiment.

The Distance Scale:

Galactic Bulge – LMC – SMC. *

A. Udalski¹

¹Warsaw University Observatory, Al. Ujazdowskie 4, 00-478 Warszawa,
Poland
e-mail: udalski@sirius.astrouw.edu.pl

ABSTRACT

We analyze the mean luminosity of three samples of field RRab Lyr stars observed in the course of the OGLE microlensing experiment: 73 stars from the Galactic bulge and 110 and 128 stars from selected fields in the LMC and SMC, respectively. The fields are the same as in the recent distance determination to the Magellanic Clouds with the red clump stars method by Udalski *et al.* (1998). We determine the relative distance scale $d_{GB}^{RR} : d_{LMC}^{RR} : d_{SMC}^{RR}$ equal to: $(0.194 \pm 0.010) : 1.00 : (1.30 \pm 0.08)$.

We calibrate our RR Lyr distance scale with the recent calibration of Gould and Popowski (1998) based on statistical parallaxes. We obtain the following distance moduli to the Galactic bulge, LMC and SMC: $m - M = 14.53 \pm 0.15$, $m - M = 18.09 \pm 0.16$ and $m - M = 18.66 \pm 0.16$ mag.

We use the RR Lyr mean V -band luminosity at the Galactic bulge metallicity as the reference brightness and analyze the mean, I -band luminosity of the red clump stars in objects with different ages and metallicities. We add to our analysis the metal poor Carina dwarf galaxy which contains old RR Lyr stars and intermediate age red clump population. We find a weak dependence of the mean red clump brightness on metallicity and we calibrate its zero point with the nearby local red clump stars measured by Hipparcos: $M_I^{RC} = (0.09 \pm 0.03) \times [\text{Fe}/\text{H}]^{RC} - 0.23 \pm 0.03$. Our revised red clump distance moduli to the Galactic bulge, LMC and SMC are $m - M = 14.53 \pm 0.06$, $m - M = 18.13 \pm 0.07$ and $m - M = 18.63 \pm 0.07$ mag, respectively. The distance modulus to the Carina galaxy is $m - M = 19.84 \pm 0.07$ mag. Excellent agreement of RR Lyr and red clump distances which have independent absolute calibrations confirms the short distance scale to the LMC.

*Based on observations obtained with the 1.3 m Warsaw telescope at the Las Campanas Observatory of the Carnegie Institution of Washington.

1 Introduction

The distance scale to the Magellanic Clouds is one of the most important problem of the modern astrophysics. In particular the distance to the Large Magellanic Cloud is a standard distance to which the extragalactic distance scale based on the Cepheid period-luminosity (P–L) relation is tied. Therefore any error in determination of the LMC distance propagates immediately to the extragalactic distances, to any value which is scaled by distance and also to the Hubble constant. Thus, precise determination of the LMC distance is of the greatest importance.

Unfortunately the distance to the LMC has for a long time been a subject of controversies. The most widely accepted "long" distance scale, $m - M \approx 18.50$ mag, was also adopted by the HST Extragalactic Distance Scale team. The "long" distance scale to the LMC is based mostly on the Cepheid P–L relation determinations (Madore and Freedman 1998) and some determinations from the supernova SN1987A light echo (Panagia *et al.* 1997).

On the other hand observations of other standard candle – RR Lyr stars – seem to favor much shorter distance to the LMC, $m - M \approx 18.3$ mag. (Layden *et al.* 1996). Such a "short" scale also seems to be preferred by reanalysis of the supernova SN1987A echo (Gould and Uza 1998).

The distance to the Small Magellanic Cloud is poorly known because observations of this galaxy with modern techniques are rare. The widely accepted SMC distance modulus is $m - M = 18.94$ mag from the Cepheid P–L relation (Laney and Stobie 1994).

Recently Udalski *et al.* (1998) employed a new technique of distance determination, proposed by Paczyński and Stanek (1998), to determine distances to the Magellanic Clouds using the mean *I*-band luminosity of the red clump stars as a standard candle. The red clump is an equivalent of the horizontal branch for intermediate population (age 2–10 Gyr) He-burning stars and is present in galaxies or clusters possessing such a population of stars.

The main advantage of the red clump stars method is that it gives a possibility of precise determination of the mean red clump luminosity, as the red clump stars are very numerous. Moreover, the red clump stars are also very numerous in the solar neighborhood and therefore the method can be calibrated very precisely with nearby stars for which parallaxes were measured with high precision by the Hipparcos satellite. No other standard candle calibration is based on direct measurements of hundreds of individ-

ual stars with precision better than 10%. Thus the red clump, single-step method seems to be potentially the most precise technique of distance determination used so far.

Udalski *et al.* (1998) found $m - M = 18.08 \pm 0.03 \pm 0.12$ mag and $m - M = 18.56 \pm 0.03 \pm 0.06$ mag for the LMC and SMC, respectively (errors are statistical and systematic, mostly from interstellar extinction uncertainty, respectively). Stanek, Zaritsky and Harris (1998) fully confirmed results of Udalski *et al.* (1998). Using independent photometry they obtained the distance modulus to the LMC equal to $m - M = 18.07 \pm 0.03 \pm 0.09$ mag reducing the systematic error by using accurate maps of interstellar extinction of their fields.

The most controversial assumption of the red clump method is the constant mean I -band brightness of the red clump stars. Paczyński and Stanek (1998), Udalski *et al.* (1998) and Stanek, Zaritsky and Harris (1998) discussed in detail the evidences in support of such an assumption, at least in the first approximation. On the other hand Cole (1998) suggested large, reaching ≈ 0.6 mag, variations of the mean red clump magnitude resulting from population differences (age, metallicity) in different objects. He attempted to calibrate the mean absolute, I -band magnitude of the red clump stars based on evolutionary models of the red clump stars and formation history of the Magellanic Clouds. Girardi *et al.* (1998) analyzed evolutionary models of the red clump stars and found the difference of $\Delta M_I = -0.235$ mag between the absolute brightness of the red clump in the LMC and local Hipparcos measured sample. This theoretical approach involves, however, many difficult to verify and often controversial assumptions like mass loss, helium content, stars formation rate etc.

In this and subsequent papers of this series we propose another, fully empirical approach to the problem of verification how much population effects can affect the mean I -band luminosity of the red clump stars. In this paper we present and analyze large samples of RR Lyr stars from the LMC and SMC obtained as a by-product of the second phase of the Optical Gravitational Lensing Experiment, OGLE-II, (Udalski, Kubiak and Szymański 1997). The samples come from the same fields which were analyzed with the red clump stars method. Together with the large sample of RR Lyr stars from the Baade's Window region of the Galactic bulge obtained during the first phase of the OGLE experiment, OGLE-I, we derive the relative RR Lyr distance scale between the Galactic bulge, LMC and SMC and determine absolute distances with the best present RR Lyr calibration.

With two standard candles in objects of different ages and metallicities

(additionally we include in our analysis the Carina dwarf galaxy which contains similar mixture of different age stellar populations), we may treat the mean brightness of RR Lyr stars as a reference point and check how the mean luminosity of the red clump stars changes from object to object. We find a clear trend which allows us to recalibrate the mean absolute *I*-band magnitude of the red clump and determine revised red clump distances.

2 Observational Data

All observations of the Magellanic Cloud RR Lyr stars were obtained with the 1.3-m Warsaw telescope located at the Las Campanas Observatory which is operated by the Carnegie Institution of Washington during the second phase of the OGLE project (Udalski, Kubiak and Szymański 1997).

The SMC objects were extracted from the preliminary version of the SMC RR Lyr stars catalog which will be released later this year. Stars from the same fields which were used for the red clump distance determination were extracted, namely SMC_SC1, SMC_SC2, SMC_SC10 and SMC_SC11 (Udalski *et al.* 1998). Each of these fields cover $\approx 14' \times 56'$ on the sky. Observations spanned the period of Jun. 26, 1997 through Feb. 12, 1998. About 100–115 *I*-band observations were used for RR Lyr search. Additionally about 20–25 *V*-band observations were used for determination of the mean $V - I$ color of the RR Lyr stars. 128 RR Lyr of ab type were selected in the SMC fields.

It is important to note that one of the RR Lyr stars, SMC_SC11 101421, is located only 87 arcsec from the center of the rich cluster NGC 419. It is possible that this is just a coincidence, because the NGC 419 is a relatively young cluster with the age of about 3 Gyr (Bica, Dottori and Pastoriza 1987) and should not harbor stars as old as RR Lyr. Only the oldest cluster in the SMC, NGC 121 contains a few RR Lyr stars (Olszewski, Suntzeff and Mateo 1996). Nevertheless, because of potential consequences on our understanding of cluster population in the SMC a possibility of cluster membership of SMC_SC11 101421 should be carefully reinvestigated.

The LMC RR Lyr stars were extracted from preliminary databases of the LMC fields: LMC_SC14, LMC_SC15, LMC_SC19 and LMC_SC20. These fields were added to the main OGLE-II LMC fields at the beginning of the 1997/98 season, and therefore the number of collected observations is smaller – about 65 in the *I*-band and only 6 in the *V*-band. Observations presented in this paper cover the period Oct. 5, 1997 through Apr. 22, 1998. To avoid

differential extinction only 1/3 of each LMC field was searched – similar as for the red clump distance determination (see Table 1, Udalski *et al.* 1998). In total 110 ab type RR Lyr stars were found in the LMC fields.

All LMC and SMC fields were carefully calibrated and accuracy of the zero points of the OGLE photometry is about 0.01 mag for the SMC and 0.01–0.02 mag for the LMC fields (Udalski *et al.* 1998). Figs. 1 and 2 present sample light curves of RRab Lyr stars from the SMC and LMC, respectively, and Table 1 and 2 list basic parameters of all RR Lyr stars.

The Galactic bulge RR Lyr stars data come from the OGLE-I catalogs of periodic variable stars (Udalski *et al.* 1994, 1995a 1995b) which are available in digital form from the OGLE archive: ftp://sirius.astrowu.edu.pl/ogle/var_catalog or <http://www.astrowu.edu.pl/~ftp/ogle>. Only RRab type stars from fields BW1-8 and BWC for which interstellar extinction could be derived from Stanek (1996) extinction map, in total 73 objects, were selected. Accuracy of the zero points of the OGLE-I photometry in dense bulge fields is about 0.03 mag (Udalski *et al.* 1993). Light curves of Galactic bulge RRab stars can be found in Udalski *et al.* (1994, 1995a 1995b). Table 3 lists the most important parameters of the Galactic bulge RRab Lyr stars.

Observations of the additional object analyzed in this paper – the Carina dwarf galaxy – were obtained as a side-project of the OGLE-II experiment. *VI*-band observations of this galaxy started on Apr. 16, 1998 and are still being continued. So far about 20 *VI* images of the field centered at $\text{RA}_{2000} = 6^{\text{h}}41^{\text{m}}34^{\text{s}}$ and $\text{DEC}_{2000} = -50^{\circ}58'00''$ were collected. The data, contrary to the Magellanic Clouds driftscan mode observations, are obtained in the normal, still frame mode and cover about $14' \times 14'$ on the sky. Typical exposure times are 600 and 900 sec for *V* and *I*-band, respectively. Observations were calibrated with the measurements of several standard stars from Landolt (1992) list collected on four photometric nights. Accuracy of the zero points of the absolute photometry is about 0.015 mag. Comparison of our photometry with previous studies (location of the red clump stars - see Section 4) shows excellent agreement with Hurley-Keller, Mateo and Nemec (1998) data for the *V*-band, Smecker-Hane *et al.* (1994) *I*-band observations, and Mighell (1997) HST WFPC2 *VI*-band data.

3 RR Lyrae Distance Scale: Galactic Bulge – LMC – SMC

3.1 RR Lyrae Data

To determine the distance scale to the Galactic Bulge, LMC and SMC with RR Lyr stars we calculated the mean magnitudes of RR Lyr stars in our three samples. First, we derived the mean, I -band intensity weighted magnitudes of each star in the sample. We fitted the light curve with high order polynomials and determined the mean intensity. We checked the results by repeating the procedure with approximation of the light curve with Fourier series. Results were consistent at the 0.01 mag level.

Then we corrected the observed magnitudes for interstellar extinction. In the case of the Galactic bulge stars we used Stanek (1996) extinction maps with the zero point correction determined by Gould, Popowski and Terndrup (1998) and Alcock *et al.* (1998b). For the Magellanic Cloud fields we assumed the same extinction as for the red clump stars: $A_I = 0.33$ mag for the LMC_SC14 and LMC_SC15 fields, $A_I = 0.39$ mag for the LMC_SC19 and LMC_SC20 fields and $A_I = 0.16$ mag for the SMC fields (Udalski *et al.* 1998). Good agreement of the red clump distance to the LMC derived by Udalski *et al.* (1998) with Stanek, Zaritsky and Harris (1998) determination for other fields confirms that these estimates of extinction are correct.

In the next step we prepared histograms of the mean magnitude of the RR Lyr stars from each sample in 0.07 mag bins. In the case of the Magellanic Clouds we decided to merge samples of fields located in west- and eastward parts of each Magellanic Cloud to increase statistics (hereafter called LMC_E, LMC_W, SMC_E and SMC_W fields). Analysis of the red clump (Udalski *et al.* 1998) indicates that in the merged fields the extinction is similar which fully justifies this step. Next, we fitted a Gaussian to each sample. The mean magnitude, I_0^{RR} , its statistical error, $\sigma_{I_0}^{\text{ST}}$, systematic error, $\sigma_{I_0}^{\text{SYS}}$, dispersion of the Gaussian, σ_{RR} , and number of stars in each sample are given in Table 4. We also calculated the mean and median magnitude and standard deviation of each sample to compare with results of Gaussian modeling. Results were almost indistinguishable, only the standard deviation was in some cases about 0.01 – 0.02 mag larger due to a few outliers.

Figs. 3 and 4 present histograms with a Gaussian function fitted to the data. As can be seen from Table 4 the σ_{RR} for each sample is similar to that of the red clump stars (Udalski *et al.* 1998, Paczyński and Stanek 1998) confirming that RR Lyr stars can be used as a good standard candle. σ_{RR} for the Magellanic Cloud samples is in good agreement with that of samples from other regions of the SMC and LMC (Smith *et al.* 1992, Hazen

Table 4

The mean I -band magnitudes of RR Lyr stars

	N_*	I_0^{RR}	$\sigma_{I_0}^{\text{ST}}$	$\sigma_{I_0}^{\text{SYS}}$	σ_{RR}
GB	73	14.77	0.019	0.04	0.25
LMC_E	43	18.45	0.020	0.05	0.19
LMC_W	67	18.38	0.014	0.05	0.14
SMC_E	59	18.92	0.026	0.05	0.21
SMC_W	69	18.93	0.014	0.05	0.18

and Nemec 1992). Dispersion larger than observed in the globular clusters (typically $\sigma_{\text{RR}} \approx 0.1$ mag) can be explained, at least in part, by depth effects for the field RR Lyr stars from our samples. The mean magnitude, I_0^{RR} , is determined with larger statistical error than that of the red clump due to much smaller number of stars. However, our RR Lyr samples will be increased by order of magnitude when precise extinction maps are derived from the OGLE-II data. In this paper we limited ourselves to stars located only in fields for which the red clump stars distances were determined.

The mean I -band magnitudes of the RR Lyr samples from different lines-of-sight in the SMC are in very good agreement. There is a few hundredth of magnitude difference for the two LMC locations. It is not clear if it is real and therefore we adopt the mean as the LMC mean RR Lyr magnitude. Adopted mean I -band magnitudes of the RR Lyr stars for the Galactic bulge, LMC and SMC are listed in Table 5.

To determine the mean V -band magnitudes of RR Lyr stars which are necessary for the distance scale determination we derived the mean $V-I$ colors of our samples. Individual color measurements were obtained by subtracting the I -band magnitude calculated from the polynomial fit to the I -band light curve at the V -band observation phase from the observed V -band magnitude. Such color curves were then averaged. In the case of the LMC RR Lyr stars for which number of V -band measurements is small, the mean color is somewhat less accurate. However, our extensive tests showed that with a sample of RR Lyr as numerous as our LMC sample the mean color is practically stable when more than four individual observations per star are collected. Our color curves of the LMC fields have six observations and

therefore we estimate that the mean color error should not exceed 0.03 mag. Similar $(V - I)_0$ color of the LMC RRab Lyr stars from the NGC 2210 region ($(V - I)_0 = 0.48$ mag) was obtained by Reid and Freedman (1994).

Mean colors of the LMC and SMC RR Lyr stars were corrected for reddening using the same values as for the red clump star distance determination: $E(V - I) = 0.10$ mag for the SMC fields, 0.22 mag for the LMC_W and 0.26 mag for the LMC_E fields (Udalski *et al.* 1998). Color of each RR Lyr star from the Galactic bulge was individually corrected for reddening with Stanek (1996) extinction map before determination of the mean $(V - I)_0$ color of the sample.

Table 5
Mean V , I and $V - I$ extinction free magnitudes of RR Lyr stars

	I_0^{RR}	$\sigma_{I_0}^{\text{ST}}$	$\sigma_{I_0}^{\text{SYS}}$	$(V - I)_0^{\text{RR}}$	$\sigma_{(V - I)_0}^{\text{ST}}$	V_0^{RR}	$\sigma_{V_0}^{\text{ST}}$	$\sigma_{V_0}^{\text{SYS}}$
GB	14.77	0.02	0.04	0.64	0.02	15.41	0.03	0.06
LMC	18.41	0.02	0.05	0.45	0.03	18.86	0.04	0.08
SMC	18.93	0.02	0.05	0.48	0.02	19.41	0.03	0.08
Carina DG	19.96	0.03	0.04	0.53	0.03	20.49	0.04	0.06

Table 5 lists the mean $(V - I)_0$ color of each of our samples with its statistical error as well as the mean V_0 magnitudes of RR Lyr stars with statistical and systematic (extinction uncertainty) errors.

In Table 5 we provide also the corresponding data for the Carina dwarf galaxy, determined from our observations. These data will be used below for analysis of the red clump stars. As the number of collected observations is too small to perform a reasonable search for RR Lyr stars in our Carina field, we decided to limit ourselves to RR Lyr stars detected in our field by Saha, Monet and Seitzer (1986). We identified 15 RRab Lyr stars and determined their mean V and I -band magnitudes by averaging their intensities. Then we corrected the mean magnitudes for interstellar extinction assuming the reddening to the Carina dwarf galaxy equal to $E(V - I) = 0.08 \pm 0.02$ (Mighell 1997) and standard relations between extinction in the V and I -bands and $E(V - I)$.

The important question when comparing objects from different locations is completeness of the sample, especially when statistics are not large and

any bias due to incompleteness may lead to gross error. In the case of the Galactic bulge, which RR Lyr stars are much brighter and light curves determined with very good precision the situation is relatively simple. Tests of completeness of the OGLE-I catalogs performed on the overlapping regions of a few fields showed that completeness for RR Lyr stars is practically 100% (Udalski *et al.* 1995b). We excluded from our Galactic bulge sample of RRab stars seven objects for which extinction could not be determined from the Stanek (1996) map.

In the case of the Magellanic Clouds the chance of overlooking some faint 19-th magnitude objects is larger because of much more noisy light curves. However, the RRab Lyr stars which are large amplitude (> 0.4 mag) variable stars, should be rather easily detectable down to $I \approx 20$ mag. Although tests of the completeness of the OGLE-II variable stars catalogs have not been performed yet, we might estimate that the completeness for RRab type stars is also high and close to 100%.

Smith *et al.* (1992) presented results of the search for variable stars on photographic plates covering $1^\circ \times 1.3^\circ$ in the north-eastern part of the SMC. They found 17 RRab type stars and estimated completeness of the search to be 68% (25 stars expected on the entire field). The Smith *et al.* (1992) field overlaps slightly with our eastern fields where we detected 59 RRab stars. Simple recalculation of the area of Smith *et al.* (1992) field and OGLE-II eastern, SMC_E, fields (0.44 square degree) leads to 174 RRab-type objects expected in the 1.3 square degree region of similar stellar density as OGLE-II eastern fields. The Smith *et al.* (1992) field, located farther to the North than OGLE-II fields, has certainly much lower stellar density – by a factor of 3–5 as indicated from our tests performed on the Digitized Sky Survey images. Therefore we may conclude that our sample of the SMC RR Lyr stars is reasonable complete, and Smith *et al.* (1992) estimate of completeness is likely underestimated. For the LMC fields, in which RRab stars are on average 0.4 mag brighter, the completeness of our samples of RR Lyr stars should be even better.

Completeness of the Carina dwarf galaxy RR Lyr sample is probably a little worse. We checked position of our 15 stars on the color-magnitude diagram (CMD) of the Carina dwarf galaxy (Fig. 5) and found about 50% more stars in the region of horizontal branch which is occupied by our RR Lyr stars. However, the mean magnitudes of these extra stars are similar to those of stars from our sample and we are convinced that our present sample is representative enough for the Carina galaxy. The mean V and I -band magnitudes of the Carina dwarf galaxy RR Lyr stars will be refined when the

final RR Lyr search in our field is completed but it is unlikely that present figures will change by more than 0.02 mag.

3.2 Relative Distance Scale $d_{GB}^{RR} : d_{LMC}^{RR} : d_{SMC}^{RR}$ from RR Lyr Stars

Before we proceed to determination of the distance scale with the RR Lyr stars an important problem of constancy of the mean absolute magnitudes of RR Lyr stars in different stellar populations should be considered. It is generally accepted that the V -band absolute magnitude of RR Lyr stars is a linear function of metallicity with the slope equal to 0.15–0.20 mag/dex. (Carney, Storm and Jones 1992, Skillen *et al.* 1993). The most controversial point of this relation is its zero point. For the rest of the paper we assume the following relation between the mean absolute V -band magnitude of RR Lyr stars and metallicity:

$$M_V^{RR} = (0.18 \pm 0.03) \times [\text{Fe}/\text{H}]^{RR} + \text{const} \quad (1)$$

It should be noted that such a relation was derived based on observations of RR Lyr stars from the Galaxy. We assume, as it is generally accepted, that it holds also in other galaxies like the Magellanic Clouds or the Carina dwarf galaxy. This is always a source of some uncertainty but the problem concerns all standard candles which are usually calibrated in our Galaxy and it is assumed that they share the same properties in other objects.

What is the mean metallicity of our samples? In general all our samples contain the field RR Lyr stars which have larger metallicities than those found in globular clusters. For the Galactic bulge sample the situation is clear – Walker and Terndrup (1991) carried out a high quality spectroscopic survey and determined the mean metallicity of the Baade's Window RR Lyr stars (59 star sample) equal to $[\text{Fe}/\text{H}]^{RR} = -1.0$ with small dispersion: 0.16 dex. Similar result from Fourier analysis of the OGLE-I RR Lyr stars light curves, $[\text{Fe}/\text{H}]^{RR} = -1.14 \pm 0.24$, was obtained by Morgan, Simet and Borgenquist (1998).

Little, however, is known about metallicities of field RR Lyr stars in the Magellanic Clouds (*cf.* Olszewski, Suntzeff and Mateo 1996). Good quality, spectroscopic surveys of these stars have yet to be done, which now, with big telescopes and huge samples of these objects emerging as by-products of the microlensing searches, can easily be obtained.

In general it seems that the field RR Lyr stars in the Magellanic Clouds are more metal rich than those from globular clusters, similarly as in the

Galaxy. Previous metallicity estimates range from -1.3 dex to -1.8 dex (Alcock *et al.* 1996, Hazen and Nemec 1992) for different fields in the LMC and from -1.6 dex to -1.8 dex for the SMC fields (Smith *et al.* 1992, Butler *et al.* 1982). Therefore we adopted metallicity equal to -1.6 ± 0.2 dex for the LMC and -1.7 ± 0.2 dex for the SMC RR Lyr stars.

The mean period of the RR Lyr stars is used often as an indicator of the metallicity of the sample. The mean periods of our samples are 0.549, 0.571 and 0.581 day for the Galactic bulge, LMC and SMC samples, respectively. Although deviations from the relation "mean period" – metallicity can be large in individual cases, these figures are consistent with metallicities adopted in our study. We stress again that a good metallicity survey of Magellanic Clouds RR Lyr stars would be of great importance to clarify the problem.

The metallicity of RR Lyr stars in Carina dwarf galaxy is estimated to be -2.2 dex (Smecker-Hane *et al.* 1994).

Table 6

Mean V -band brightness of RR Lyr stars reduced to the Galactic bulge metallicity

	V_0^{RR}	$\sigma_{V_0}^{\text{ST}}$	$\sigma_{V_0}^{\text{SYS}}$	$V_0^{\text{RR@GB}}$	$\sigma_{\text{RR@GB}}^{\text{SYS}}$	$[\text{Fe}/\text{H}]^{\text{RR}}$
GB	15.41	0.03	0.06	15.41	0.07	-1.0 ± 0.1
LMC	18.86	0.04	0.08	18.97	0.09	-1.6 ± 0.2
SMC	19.41	0.03	0.08	19.54	0.09	-1.7 ± 0.2
Carina DG	20.49	0.04	0.06	20.71	0.08	-2.2 ± 0.2

Combining the metallicity differences with the absolute magnitude-metallicity relation we find that, on average, the LMC, SMC and Carina dwarf galaxy samples should be about 0.11 ± 0.04 mag, 0.13 ± 0.04 mag and 0.22 ± 0.05 mag brighter than the Galactic bulge one, respectively (Eq. 1). In Table 6 we present the mean V -band magnitudes of the LMC, SMC and Carina RR Lyr samples reduced to the Galactic bulge metallicity, $V_0^{\text{RR@GB}}$, by applying above corrections.

The possible systematic errors, $\sigma_{V_0}^{\text{SYS}}$, of the mean magnitudes of our RR Lyr samples come mostly from extinction uncertainties. In the case of the Galactic bulge the Stanek (1996) map zero point was corrected with two independent methods (Gould, Popowski and Terndrup 1997, and Alcock *et*

al. 1998b) yielding exactly the same corrections, thus indicating that the average systematic V -band extinction error of our sample should be smaller than 0.06 mag. With uncertainties of the zero point of the photometry the total systematic uncertainty is 0.07 mag. In the case of the Magellanic Clouds extinction error should not exceed 0.08 mag. Combining this with uncertainty of metallicity difference between our Magellanic Cloud samples and the Galactic bulge sample we obtain the total systematic error, $\sigma_{RR@GB}^{SYS}$, to be 0.09 mag for both Magellanic Clouds. For the Carina dwarf galaxy the V -band extinction uncertainty is 0.06 mag, and $\sigma_{RR@GB}^{SYS}$ 0.08 mag.

Now, we can proceed to determination of the relative distance scale resulting from RR Lyr photometry. Taking the LMC distance as an unit, we find the following relative distance scale $d_{GB}^{RR} : d_{LMC}^{RR} : d_{SMC}^{RR}$

$$(0.194 \pm 0.010) : 1.00 : (1.30 \pm 0.08)$$

3.3 Absolute Calibration of the Relative RR Lyrae Distance Scale

The absolute calibration of RR Lyr stars has been a subject of many disputes and controversies for many years. The RR Lyr stars are too far to have reliable direct parallaxes even from the Hipparcos satellite. At present the most reliable calibration seems to come from statistical parallaxes derived from measurements of about hundred and fifty stars with both ground based and Hipparcos proper motions (series of papers by Gould and Popowski 1998 and references therein). After very careful analysis of possible systematic errors of their large RR Lyr stars sample, Gould and Popowski (1998) derive the mean absolute magnitude of the RR Lyr stars to be equal $M_V^{RR} = 0.77 \pm 0.13$ at metallicity $[\text{Fe}/\text{H}]^{RR} = -1.6$ dex. Similar results but from smaller sample were also obtained by Fernley *et al.* (1998).

We may attempt to calibrate our RR Lyr distance scale using Gould and Popowski (1998) calibration and our Galactic bulge RR Lyr sample for which we have precise metallicity determination from Walker and Terndrup (1991) and to which metallicity the mean V -band magnitudes of RR Lyr stars in our objects were reduced (Table 6).

For the metallicity of the Baade's Window RR Lyr variables equal to -1.0 dex and the mean slope of the M_V^{RR} – metallicity relation for RR Lyr stars equal to 0.18 mag/dex (Eq. 1) we obtain $M_V^{RR} = 0.88 \pm 0.14$ mag. Distance moduli are then derived by subtracting that value from the mean V -band brightness reduced to the bulge metallicity (column 4 Table 6) and

are listed in Table 7. The main component in the total error budget, σ^{TOT} , comes from uncertainty of the Gould and Popowski (1998) calibration with much smaller contribution from statistical error of the mean V -band magnitude of our RR Lyr samples and its systematic uncertainty.

Table 7
RR Lyr distances

	$[\text{Fe}/\text{H}]^{\text{RR}}$	$m - M$	σ^{TOT}	d [kpc]
GB	-1.0	14.53	0.15	8.1
LMC	-1.6	18.09	0.16	41.5
SMC	-1.7	18.66	0.16	54.0
Carina DG	-2.2	19.83	0.15	92.5

4 Red Clump Distance Scale: Galactic Bulge – LMC – SMC

Recent determinations of distances to the Galactic bulge (Paczyński and Stanek 1998), LMC (Udalski *et al.* 1998, Stanek, Zaritsky and Harris 1998) and SMC (Udalski *et al.* 1998) with a newly developed red clump stars method (Paczyński and Stanek 1998) enable us to compare the distance scale to all three objects obtained with the RR Lyr stars in the previous Section with the red clump distances. Our selection of the same lines-of-sight for the RR Lyr and the red clump determinations makes both similarly affected by possible systematic errors resulting from interstellar extinction making such a comparison more reliable. The statistical errors are almost an order of magnitude smaller for the red clump stars which are much more numerous than RR Lyr stars but even for the latter they are of the order of only 0.03 mag, much smaller than systematic errors.

In Table 8 we list the mean I -band, extinction free magnitudes of the red clump stars, I_0^{RC} , for objects to which the red clump method has already been applied: the Galactic bulge, LMC, SMC and M31 (Paczyński and Stanek 1998, Udalski *et al.* 1998, Stanek and Garnavich 1998) with their

Table 8
Red clump mean luminosity

	I_0^{RC}	$\sigma_{I_0}^{\text{ST}}$	$\sigma_{I_0}^{\text{SYS}}$	$[\text{Fe}/\text{H}]^{\text{RC}}$	References
GB	14.32	0.009	0.04	$+0.2 \pm 0.2$	Paczyński and Stanek (1998)
LMC	17.85	0.004	0.05	-0.6 ± 0.2	Udalski <i>et al.</i> (1998)
SMC	18.33	0.003	0.05	-0.8 ± 0.2	Udalski <i>et al.</i> (1998)
M31 Halo	24.24	0.010	0.05	-0.5 ± 0.2	Stanek and Garnavich (1998)
M31 Cluster	24.22	0.013	0.05	-0.7 ± 0.2	Stanek and Garnavich (1998)
Carina DG	19.44	0.005	0.04	-1.9 ± 0.2	this paper

statistical, $\sigma_{I_0}^{\text{ST}}$, and systematic, $\sigma_{I_0}^{\text{SYS}}$, errors.

We added to our list of analyzed objects the Carina dwarf galaxy which contains both old and intermediate age populations of stars similar to the Magellanic Clouds. The Carina galaxy is also very metal poor which makes it ideal for testing stability of the red clump luminosity in different stellar environments.

In Table 8 we provide the mean I -band magnitude of the red clump of the Carina dwarf galaxy determined in similar way as for the LMC and SMC (Udalski *et al.* 1998). Fig. 5 presents the I vs. $(V - I)$ CMD of the Carina galaxy based on our observations. Fig. 6 shows the luminosity function histogram in 0.04 mag bins of stars in the Carina galaxy red clump region and the Gaussian function with second order polynomial background fitted to the data (Udalski *et al.* 1998). We assumed the I -band extinction equal to 0.12 ± 0.03 (Mighell 1997) and we selected stars from the range: $0.7 < (V - I)_0 < 0.9$ mag and $20.5 < I_0 < 18.5$, in total 696 stars. The color range is somewhat different than in previous determinations of the red clump mean luminosity, but because of low metallicity and compactness of the red clump in the Carina galaxy its large part falls blueward of the blue limit of previous determinations. For comparison we also determined the mean magnitude of the red part of the red clump falling in the range $0.8 < (V - I)_0 < 0.9$ mag. The mean magnitude of such a sample was 19.42 mag *i.e.*, 0.02 mag brighter than the mean magnitude of the entire clump.

4.1 *I*-band Mean Luminosity of the Red Clump Stars

The most controversial point of the red clump stars method of distance determination is the assumption of the same mean luminosity of the red clump stars in populations of different age, metallicity etc. Empirical evidences like constant *I*-band magnitude of the red clump stars over the wide range of observed colors (Paczyński and Stanek 1998), similar distance determination for different population fields in M31 (Stanek and Garnavich 1998) seem to suggest that this is indeed the case. Also some models of the red clump stars confirm weak dependence of the red clump luminosity on age (Castellani, Chieffi and Straniero 1992). On the other hand models of Bertelli *et al.* (1994) predict much stronger dependence of the red clump luminosity on metallicity and age reaching up to a few tens of magnitude for the populations as different as our local environment and Magellanic Cloud stars. Cole (1998) suggested that population effects can account even for 0.6 mag for different stellar populations. Girardi *et al.* (1998) obtained about 0.24 mag brighter red clump in the LMC than for stars from solar neighborhood. Thus it is very important to verify empirically how well the assumption of the constant mean luminosity of the red clump holds.

Having two potential standard candles in our four different objects, Galactic bulge, LMC, SMC and Carina dwarf galaxy, we may compare them and assuming that the RR Lyr are, as commonly accepted, good standard candles check how stable is the mean *I*-band magnitude of the red clump stars in different populations. It should be stressed here, that although both RR Lyr stars and the red clump giants have similar internal structure – both are He-core, H-shell burning stars – we compare two completely different stellar populations. The field RR Lyr stars are the old objects with small metallicities. On the other hand the red clump consists from much younger stars but with different formation histories and metallicities in all our four objects. The mean metallicity of our red clump samples covers much wider range from the metal richest Galactic bulge with metallicity ($-0.3 \div 0.3$) dex (*cf.* Table 6 Minitti *et al.* 1995), through the LMC ($-0.8 \div -0.5$) dex (Bica *et al.* 1998) and SMC ($-1.0 \div -0.7$) dex (Olszewski, Suntzeff and Mateo 1996) to Carina dwarf galaxy -1.9 dex (Mighell 1997). Also other evidences like different spatial distribution of both kinds of stars in the Galactic bulge strongly suggest completely different populations – the red clump stars are grouped in the bar (Stanek *et al.* 1997), while the RR Lyr stars belong to the spherical halo objects (Alcock *et al.* 1998a).

If we assume that the mean *V*-band magnitude of the RR Lyr stars

reduced to the same – Galactic bulge – metallicity is constant, we might treat the mean reduced magnitudes of the RR Lyr stars (column 4 of Table 6) as a reference point. This assumption is supported by many evidences like *e.g.*, similar luminosity of globular cluster and field RR Lyr stars (Catelan 1998).

Table 9
Red Clump minus RR Lyr luminosity

	$I_0^{\text{RC}} - V_0^{\text{RR@GB}}$	$\sigma_{\text{RC-RR@GB}}^{\text{TOT}}$	$[\text{Fe}/\text{H}]^{\text{RC}}$
GB	-1.09	0.04	$+0.2 \pm 0.2$
LMC	-1.12	0.06	-0.6 ± 0.2
SMC	-1.21	0.06	-0.8 ± 0.2
Carina DG	-1.27	0.07	-1.9 ± 0.2

Differences between the mean I -band brightness of the red clump stars and reduced to the bulge metallicity, mean V -band luminosity of the RR Lyr stars, $I_0^{\text{RC}} - V_0^{\text{RR@GB}}$, with their total errors, $\sigma_{\text{RC-RR@GB}}^{\text{TOT}}$ are listed in Table 9. The total error includes statistical error, systematic – $E(V - I)$ reddening – error and uncertainty of the RR Lyr brightness-metallicity relation (Eq. 1).

Fig. 7 presents the differences as a function of metallicity of the red clump stars, $[\text{Fe}/\text{H}]^{\text{RC}}$. There is a clear trend of larger difference for metal poorer objects suggesting somewhat brighter red clump in metal deficient objects. If our reference point defined by the RR Lyr mean V -band magnitude at the Galactic bulge metallicity is correct we observe an apparent correlation between the mean red clump magnitude and metallicity of the object. We can therefore attempt to calibrate the red clump mean magnitude and the best, linear fit to the data is:

$$M_I^{\text{RC}} = (0.09 \pm 0.03) \times [\text{Fe}/\text{H}]^{\text{RC}} + \text{const.} \quad (2)$$

We are only interested in the slope of this relation, as we will calibrate it very precisely in the next Subsection. It should be noted that despite the fact that our calibration is based on four points only, each of these points is very well determined – based on thousands of red clump stars and tens

of RR Lyr stars. They also cover a very wide range of metallicities. We hope that in the future more points can be added to this calibration when for instance RR Lyr stars are detected in the Leo I dwarf galaxy (Lee *et al.* 1993) or similar objects.

The slope of the I -band brightness-metallicity relation for the red clump stars we derived is much smaller than analogous slope of the mean V -band brightness-metallicity relation for RR Lyr stars (Eq. 1) indicating much weaker dependence of red clump luminosity on metallicity.

The dependence of the red clump I -band luminosity on the metallicity was expected from some evolutionary models of the red clump stars (*e.g.*, Bertelli *et al.* 1994, Cole 1998). For example, Cole (1998) obtained 0.21 ± 0.07 mag/dex slope of the brightness-metallicity relation for the red clump stars. Girardi *et al.* (1998) predicted the difference of 0.24 mag between the absolute luminosity of the red clump in the LMC and the local Hipparcos sample. Our difference of the red clump absolute magnitude between the LMC and the local Hipparcos sample is only 0.05 mag and the slope of brightness-metallicity relation 0.09 mag/dex. Thus, it seems that theoretical predictions are by factor of at least two too large comparing with our empirical determination. It should be, however, noted that the slope of the red clump stars relation is tied with the slope of the RR Lyr relation in the sense that larger slope of RR Lyr relation means larger slope for the red clump relation and *vice versa*. If, for instance, we assume that the slope of the RR Lyr brightness-metallicity relation (Eq. 1) is as large as 0.37 mag/dex, as sometimes suggested (Feast, 1997), the slope of the red clump relation would increase to 0.20 mag/dex resulting in somewhat longer distances to our objects than derived in the next Subsection (distance moduli larger by ≈ 0.08 mag for the Magellanic Clouds and ≈ 0.2 mag for the Carina galaxy).

4.2 Absolute Calibration of the Red Clump Luminosity

In the case of the red clump stars the absolute calibration can be obtained with very good precision and practically the red clump stars are the only standard candle calibrated *via* a direct measurement. Paczyński and Stanek (1998) proposed a local red clump giants with precise parallaxes (accuracy better than 10%) measured by Hipparcos as a calibrator of the red clump distances. The large number of such stars, precise distances and photometry make them ideal for that purpose. The best calibration from the distance ($d < 70$ pc) limited sample (> 200 objects) is $M_I^{\text{RC}} = -0.23 \pm 0.03$ mag

(Stanek and Garnavich 1998). Assuming that the local sample mean metallicity is equal to solar, $[\text{Fe}/\text{H}]^{\text{RC}} = 0.0$, we may use the Hipparcos data to determine the zero point of our brightness-metallicity relation for the red clump stars:

$$M_I^{\text{RC}} = (0.09 \pm 0.03) \times [\text{Fe}/\text{H}]^{\text{RC}} - 0.23 \pm 0.03. \quad (3)$$

T a b l e 10
Red clump distances

	$[\text{Fe}/\text{H}]^{\text{RC}}$	Old $m - M$	Revised $m - M$	σ^{TOT}	d [kpc]
GB	+0.2	14.55	14.53	0.06	8.1
LMC	-0.6	18.08	18.13	0.07	42.3
SMC	-0.8	18.56	18.63	0.07	53.2
M31 halo	-0.5	24.47	24.52	0.07	802
M31 cluster	-0.7	24.45	24.51	0.07	798
Carina DG	-1.9	—	19.84	0.07	92.9

In Table 10 we list the new, revised distance moduli to objects to which they were determined before with the assumption of constant I -band magnitude of the red clump. Old distances are also included. σ^{TOT} corresponds to the total error of the distance determination: statistical, calibration and systematic errors. Table 10 also contains distance modulus to the metal poor Carina dwarf galaxy for comparison of the red clump method distance determination with other methods.

As can be seen from Table 10, the differences between the old and new distances are small, at most of the order of 0.05–0.07 mag because of small overall metallicity range of objects analyzed so far and small slope of the brightness-metallicity relation for the red clump stars. Much larger discrepancy, reaching ≈ 0.2 mag would be expected for the metal poor objects. It should be noted here that the new absolute distances, although calibrated independently of the RR Lyr distances, are somewhat dependent on RR Lyr stars. The brightness-metallicity relation for RR Lyr was assumed to bring the RR Lyr luminosities to the reference Galactic bulge metallicity brightness, for determination of the brightness-metallicity relation of the red clump

stars.

The distance modulus to the most important astrophysical object, the LMC, can be now determined very precisely, as the calibration error is small – about 0.04 mag, and systematic error can be reduced to 0.05 mag based on similar results of Udalski *et al.* (1998) and Stanek, Zaritsky and Harris (1998). Thus, our final distance modulus of the LMC is $m - M = 18.13 \pm 0.07$ mag. Revised distance moduli to the SMC and Galactic bulge are $m - M = 18.63 \pm 0.07$ mag and $m - M = 14.53 \pm 0.06$ mag, respectively.

Finally, we can compare the distance to the metal poor Carina dwarf galaxy determined with the revised red clump method with other results. The most recent determination of the distance to the Carina galaxy was obtained by Michell (1997) who determined the distance modulus equal to $m - M = 19.87 \pm 0.11$ mag. This determination is in excellent agreement with both our results – from the red clump and RR Lyr stars.

5 Discussion

We analyzed and determined the distance scale to three objects, the Galactic bulge, LMC and SMC, with two different standard candles: the red clump stars and RR Lyr variables, based on the huge databases of photometric measurements from the OGLE-II microlensing search. From the photometry of RR Lyr stars in the Galactic bulge, LMC and SMC we obtain the following relative distance scale $d_{GB}^{RR} : d_{LMC}^{RR} : d_{SMC}^{RR}$

$$(0.194 \pm 0.010) : 1.00 : (1.30 \pm 0.08).$$

This scale is based on direct photometric measurements with an appropriate metallicity corrections applied to each sample of stars and is independent of absolute calibration.

The first test which we can immediately perform is the verification of the "long" distance scale to the LMC, $m - M = 18.50$, *i.e.*, 50.1 kpc. If we assume that distance to the LMC, then the distance to the Galactic bulge must be 9.72 ± 0.50 kpc. This value seems to be in contradiction with practically all present determinations of the distance to the Galactic center, 8.0 ± 0.5 kpc (Reid 1993). On the other hand even that crude calibration – the mean distance to the Galactic center – suggests "short" distance scale to the LMC – about 41.2 kpc ($m - M = 18.08$ mag).

Measurements of two standard candles in the same lines-of-sight: to the Galactic bulge, LMC, SMC and Carina dwarf galaxy enable us to compare

them and – adopting the RR Lyr luminosity as a reference point – to analyze the mean luminosity of the red clump stars in objects with different ages, star formation histories and metallicities. Moreover, our reference point, RR Lyr stars, belong to completely different, much older, population with different metal content and kinematic properties. This fact combined with good standard candle properties of RR Lyr stars – small dispersion of the mean absolute luminosity as observed in globular clusters, similar properties of RR Lyr stars in different environments (cluster and field objects) and well constrained slope of the brightness-metallicity dependence – make RR Lyr stars a very good reference for the red clump mean brightness comparison.

Our analysis shows that the assumption of the constant red clump luminosity holds with accuracy of about 0.09 mag for populations differing with mean metallicity by up to 1 dex. We derive a calibration of the red clump mean *I*-band magnitude *vs.* metallicity based on analysis of four objects, the Galactic bulge, LMC, SMC and Carina dwarf galaxy, covering large range of metallicities: $+0.2 \div -1.9$ dex. The slope of this calibration seems to be well constrained, the zero point can be determined very precisely based on the local, Hipparcos measured red clump stars. The calibration is thus much more reliable than that of any other standard candle. The red clump stars method can be now safely applied even to very metal poor objects.

Our empirical calibration of the red clump mean *I*-band magnitude shows much smaller dependence on metallicity than resulting from theoretical models (Cole 1998, Girardi *et al.* 1998). This discrepancy can be a result of many difficult to verify assumptions (*e.g.*, star formation history in the Magellanic Clouds, helium content) used for modeling of the red clump.

We also do not see any significant dependence of the red clump luminosity on age as residuals from our brightness-metallicity relation are negligible. Models predict much brighter red clump for younger stars, younger than ≈ 2 Gyr, (Girardi and Bertelli 1998) which is indeed observed in the LMC young clusters. Brighter, young red clump stars are also found as the vertical extension of the red clump in the field color-magnitude diagrams (Zaritsky and Lin 1997, Beaulieu and Sackett 1998, Udalski *et al.* 1998). For older stars luminosity is practically age independent which indicates that the vast majority of stars in the red clump of the analyzed objects, Galactic bulge, LMC, SMC and Carina galaxy must be older than 2 Gyr. Empirical tests of the red clump brightness-age relation will be presented and discussed in the next paper of the series.

In Table 10 we present revised distance moduli to the Magellanic Clouds and Galactic bulge obtained with the modified red clump method. The

differences between the old and revised distance moduli are small, not exceeding 0.07 mag. The revised red clump method confirms the previous result of the "short" distance scale to the LMC (Udalski *et al.* 1998, Stanek, Zaritsky and Harris 1998).

The absolute distances to the Galactic bulge, LMC, SMC and Carina galaxy can also be independently determined with the RR Lyr relative distance scale and the absolute magnitude calibration for RR Lyr stars. Such a calibration is less accurate than calibration of the red clump method, as even the closest galactic RR Lyr stars are too distant to be measured directly. The most reliable calibration of the RR Lyr absolute magnitude of Gould and Popowski (1998) gives the distance moduli listed in Table 7. They are in excellent agreement with determination from the red clump stars method.

Although our calibration of the brightness-metallicity relation of the red clump stars based on the RR Lyr stars as the reference point makes the relative distance scales determined from the red clump and RR Lyr stars fully dependent, we have to stress that the absolute calibrations of both distance indicators are absolutely independent. The red clump calibration is based on the nearby red clump stars measured by the Hipparcos satellite, while the calibration of the RR Lyr stars comes from much older, metal deficient stars, belonging to other population and located in completely different parts of the Galaxy. Also the methods of calibration are completely independent: trigonometric parallaxes for the red clump stars and statistical parallaxes for RR Lyr stars. Absolute distances determined by both, so different distance indicators are, however, in excellent agreement which strongly confirms that our approach is correct.

Very good agreement of the distance determination to the LMC with the red clump stars method and RR Lyr stars, is a strong argument in favor of the "short" distance scale to the LMC. From other reliable distance indicators only the Cepheid P-L relation seems to favor the "long" distance scale. As discussed by Udalski *et al.* (1998) and Stanek, Zaritsky and Harris (1998) we suspect that the Cepheid P-L relation requires significant revision. For instance, Sekiguchi and Fukugita (1998) suggested that metallicity effects may bring the Cepheid P-L based distance to the LMC to "short" values.

We believe that our relative distance scale to the Galactic bulge, LMC and SMC, as well as absolutely calibrated distances determined with two distance indicators belonging to different populations of stars and calibrated independently are at present the most accurate distance determinations to these objects. However, we have to stress here that independent determinations with other precise techniques are still of great importance. Well

detached eclipsing binary systems seem to be the most promising candidates for accurate testing the distance scale (Paczyński 1997). It is a bit distressing that at the end of 20th century one of the most important topics of the modern astrophysics, determination of the distance to the LMC – the milestone for the extragalactic distance scale – is a subject of controversy reaching as much as 15%.

Acknowledgements. We would like to thank Prof. Bohdan Paczyński for many encouraging and stimulating discussions and help at all stages of the OGLE project. We thank Drs M. Kubiak, M. Szymański and K.Z. Stanek for many remarks and comments. Part of observations of the Carina galaxy analyzed in this paper was carried out by Dr. M. Szymański. The paper was partly supported by the Polish KBN grant 2P03D00814 to A. Udalski. Partial support for the OGLE project was provided with the NSF grant AST-9530478 to B. Paczyński.

REFERENCES

Alcock *et al.* 1996, *Astron. J.*, **111**, 1146.
 Alcock *et al.* 1998a, *Astrophys. J.*, **492**, 190.
 Alcock *et al.* 1998b, *Astrophys. J.*, **494**, 396.
 Beaulieu, J.P., and Sackett, P.D. 1998, *Astron. J.*, in press, (astro-ph/9710156).
 Bertelli, G., Bressan, A., Chiosi, C., Fagotto, F., and Nasi, E. 1994, *Astron. Astrophys. Suppl. Ser.*, **106**, 275.
 Bica, E., Dottori, H., and Pastoriza, M. 1987, *Astron. Astrophys.*, **156**, 261.
 Bica, E., Geisler, D., Clariá, J.J., and Piatti, A.E. 1998, *Astron. J.*, in press, (astro-ph/9803167).
 Butler, D., Demarque, P., and Smith, H.A. 1982, *Astrophys. J.*, **257**, 592.
 Carney, B.W., Storm, J., and Jones, R.V. 1992, *Astrophys. J.*, **386**, 663.
 Castellani, V., Chieffi, A., and Straniero, O. 1992, *Astrophys. J. Suppl. Ser.*, **78**, 517.
 Catelan M. 1998, *Astrophys. J. Letters*, **495**, L81.
 Cole, A.A. 1998, *Astrophys. J. Letters*, in press, (astro-ph/9804110).
 Feast, M.W. 1997, *MNRAS*, **284**, 761.
 Fernley, J., *et al.* 1998, *Astron. Astrophys.*, **330**, 512.
 Girardi, L., and Bertelli, G. 1998, *MNRAS*, in press, (astro-ph/9801145).
 Girardi, L., Groenewegen, M.A.T., Weiss, A., and Salaris, M. 1998, *MNRAS*, submitted, (astro-ph/9805127).
 Gould, A., and Uza, O. 1998, *Astrophys. J. Letters*, **494**, L118.
 Gould, A., Popowski, P., and Terndrup, D.T. 1998, *ApJ*, **492**, 778.
 Gould, A., and Popowski, P. 1998, *Astrophys. J.*, submitted, (astro-ph/9805176).
 Hazen, M.L., and Nemec, J.M. 1992, *Astron. J.*, **104**, 111.
 Hurley-Keller, D., Mateo, M., and Nemec, J. 1998, *Astron. J.*, in press, (astro-ph/9804058).
 Landolt, A.U. 1992, *Astron. J.*, **104**, 372.
 Laney, C.D., and Stobie, R.S. 1994, *MNRAS*, **266**, 441.
 Layden, A.C., Hanson, R.B., Hawley, S.L., Klemola, A.R., and Hanley, C.J. 1996, *Astron. J.*, **112**, 2110.
 Lee M.G., Freedman, W., Mateo, M., Thompson, I., Roth, M., and Ruiz, M.T. 1993, *Astron. J.*, **106**, 1420.
 Madore, B.F., and Freedman, W.L. 1998, *Astrophys. J. Letters*, **492**, 110.
 Michell, K.J. 1997, *Astron. J.*, **114**, 1458.
 Minitti, D., Olszewski, E.W., Liebert, J., White, S.D.M., Hill, J.M., and Irwin, M.J. 1994, *MNRAS*, **277**, 1293.
 Morgan, S.M., Simet, M., and Borgenquast, S 1998, *Acta Astron.*, **48**, in press.
 Olszewski, E.W., Suntzeff, N.B., and Mateo, M. 1996, *ARA&A*, **34**, 511.
 Paczyński, B. 1997, in: "The Extragalactic Distance Scale STScI Symposium", Baltimore, Cambridge University Press, 273 (astro-ph/9608094).
 Paczyński B., and Stanek, K.Z. 1998, *Astrophys. J. Letters*, **494**, L219.
 Panagia, N., Gilmozzi, R., Kirshner, R.P., Pun, C.S.J., and Sonneborn, G. 1997, *BAAS*, **191**, 19.09.
 Reid, M.J. 1993, *ARA&A*, **31**, 345.
 Reid, N., and Freedman, W.L. 1994, *MNRAS*, **267**, 821.
 Saha, A., Monet, D.G., and Seitzer, P. 1986, *Astron. J.*, **92**, 302.
 Sekiguchi, M., and Fukugita, M. 1998, *Observatory*, in press, (astro-ph/9707229).
 Skillen, I., Fernley, J.A., Stobie, R.S., and Jameson, R.F. 1993, *MNRAS*, **265**, 301.

Smecker-Hane, T.A., Stetson, P.B., Hesser, J.E. and Lehnert, M.D. 1994, *Astron. J.*, **108**, 507.

Smith H.A, Silbermann, N.A., Baird, S.R., and Graham, J.A. 1992, *Astron. J.*, **104**, 1430., Stanek, K.Z. 1996, *Astrophys. J. Letters*, **460**, L37.

Stanek, K.Z., Udalski, A., Szymański, M., Kałużny,J., Kubiak, M., Mateo, M., and Krzemieński, W. 1997, *Astrophys. J.*, **477**, 163.

Stanek K.Z., and Garnavich, P.M. 1998, *Astrophys. J. Letters*, in press, (astro-ph/9802121).

Stanek K.Z., Zaritsky, D., and Harris, J. 1998, *Astrophys. J. Letters*, in press, (astro-ph/9803181).

Udalski, A., Kubiak, M., and Szymański, M. 1997, *Acta Astron.*, **47**, 319.

Udalski A., Szymański, M., Kałużny,J., Kubiak, M., and Mateo, M. 1993, *Acta Astron.*, **43**, 69.

Udalski, A., Szymański, M., Kałużny,J., Kubiak, M., Mateo, M., and Krzemieński, W. 1994, *Acta Astron.*, **44**, 317.

Udalski, A., Szymański, M., Kałużny,J., Kubiak, M., Mateo, M., Krzemieński, W. 1995a, *Acta Astron.*, **45**, 1.

Udalski, A., Olech, A., Szymański, M., Kałużny,J., Kubiak, M., Mateo, M., Krzemieński, W. 1995b, *Acta Astron.*, **45**, 433.

Udalski, A., Szymański, M., Kubiak, M., Pietrzyński, G., Woźniak, P., and Żebruń, K. 1998, *Acta Astron.*, **48**, 1, (astro-ph/9803035).

Walker, A.R., and Terndrup, D.M. 1991, *Astrophys. J.*, **378**, 119.

Zaritsky, D., and Lin, D.B.C. 1997, *Astron. J.*, **114**, 2545.

Figure captions

Fig. 1. Sample light curves of the RR Lyr stars from the Small Magellanic Cloud (field – SMC_SC1). Ordinate is phase (maximum of brightness corresponds to the phase 0.0) and abscissa the I -band magnitude. For each star the number from the database and period in days are also given.

Fig. 2. Sample light curves of the RR Lyr stars from the Large Magellanic Cloud (field – LMC_SC14). Ordinate is phase (maximum of brightness corresponds to the phase 0.0) and abscissa the I -band magnitude. For each star the number from the database and period in days are also given.

Fig. 3. Distribution of the I -band mean, extinction free, magnitudes of the RR Lyr stars in the Galactic bulge (Baade's Window). Bins are 0.07 mag wide.

Fig. 4. Distribution of the I -band mean, extinction free, magnitudes of the RR Lyr stars in the Magellanic Cloud fields. Bins are 0.07 mag wide.

Fig. 5. $I - (V - I)$ Color-Magnitude Diagram of the Carina dwarf galaxy. The star denotes the mean location of the RR Lyr stars.

Fig. 6. Luminosity function of the red clump stars in the Carina dwarf galaxy. Bins are 0.04 mag wide. The solid line represents the best fit of a Gaussian superimposed on the parabola function.

Fig. 7. Difference between the mean I -band magnitude of the red clump stars and the mean V -band luminosity of the RR Lyr stars reduced to metallicity of the Galactic bulge in the Galactic bulge (GB), LMC, SMC and Carina dwarf galaxy plotted as a function of metallicity of the red clump stars. The dotted line represents the best linear fit given by Eq. 2.

Table 1
RR Lyrae in the SMC fields

SMC_SCI No	α_{2000}	δ_{2000}	P [days]	T_0 [HJD]	$\langle I_0 \rangle$ [mag]	$\langle (V - I)_0 \rangle$ [mag]
66	0 ^h 36 ^m 42 ^s 78	-73°56'12".2	0.52564	2450627.37071	19.227	0.284
278	0 ^h 36 ^m 34 ^s 14	-73°55'53".1	0.63296	2450627.39925	18.929	0.570
4659	0 ^h 36 ^m 23 ^s 03	-73°46'51".0	0.56603	2450627.79256	18.779	0.467
7953	0 ^h 36 ^m 33 ^s 22	-73°38'00".8	0.63092	2450627.66134	18.777	0.504
8278	0 ^h 36 ^m 20 ^s 56	-73°37'24".1	0.63943	2450629.73919	18.870	0.542
15170	0 ^h 36 ^m 19 ^s 43	-73°25'53".0	0.41917	2450631.77014	18.755	0.459
17022	0 ^h 36 ^m 40 ^s 43	-73°19'43".1	0.64226	2450627.78219	18.765	0.499
17258	0 ^h 37 ^m 00 ^s 87	-73°20'38".6	0.49616	2450627.49295	19.172	0.469
22204	0 ^h 36 ^m 48 ^s 59	-73°10'03".0	0.55463	2450627.49350	19.143	0.506
22211	0 ^h 36 ^m 16 ^s 10	-73°09'53".2	0.61046	2450666.52024	18.884	0.544
27447	0 ^h 37 ^m 07 ^s 89	-73°56'13".8	0.62846	2450627.61124	18.756	0.434
27509	0 ^h 37 ^m 07 ^s 32	-73°54'55".8	0.56272	2450627.72267	18.962	0.478
35779	0 ^h 37 ^m 37 ^s 63	-73°39'14".6	0.58823	2450627.69660	19.019	0.438
37568	0 ^h 37 ^m 50 ^s 29	-73°36'33".9	0.57603	2450626.70932	18.775	0.424
37666	0 ^h 37 ^m 40 ^s 00	-73°35'13".5	0.66764	2450626.84656	18.950	0.523
39508	0 ^h 37 ^m 31 ^s 47	-73°32'10".8	0.68791	2450627.35842	18.722	0.511
41932	0 ^h 37 ^m 23 ^s 51	-73°27'00".6	0.52252	2450625.82636	19.053	0.391
49318	0 ^h 37 ^m 26 ^s 22	-73°14'20".0	0.51957	2450625.84970	18.914	0.437
49578	0 ^h 37 ^m 27 ^s 79	-73°14'54".9	0.41269	2450625.69539	19.346	0.446
51454	0 ^h 37 ^m 04 ^s 41	-73°10'23".2	0.65202	2450627.44833	18.599	0.470
53520	0 ^h 37 ^m 33 ^s 91	-73°06'07".7	0.57346	2450625.76295	19.049	0.415
57278	0 ^h 37 ^m 52 ^s 40	-73°55'55".9	0.57708	2450627.71200	18.842	0.469
60939	0 ^h 38 ^m 36 ^s 06	-73°47'50".2	0.58386	2450625.55823	19.037	0.496
62463	0 ^h 37 ^m 56 ^s 31	-73°45'08".8	0.58916	2450626.82731	18.958	0.532
63932	0 ^h 37 ^m 57 ^s 71	-73°43'26".9	0.58386	2450625.83031	18.542	0.448
64191	0 ^h 37 ^m 58 ^s 85	-73°43'39".5	0.52318	2450625.90891	18.933	0.415
67537	0 ^h 38 ^m 31 ^s 01	-73°35'39".6	0.61347	2450625.47035	18.986	0.469
67598	0 ^h 38 ^m 24 ^s 91	-73°35'00".5	0.60257	2450625.62523	18.909	0.516
71673	0 ^h 38 ^m 34 ^s 62	-73°28'30".0	0.60831	2450625.32503	18.656	0.395
71674	0 ^h 38 ^m 03 ^s 07	-73°28'29".2	0.61335	2450625.36187	19.069	0.416
72095	0 ^h 38 ^m 39 ^s 07	-73°27'26".0	0.54736	2450625.63563	19.055	0.391
73883	0 ^h 38 ^m 16 ^s 44	-73°24'49".2	0.42801	2450625.62528	19.096	0.404
74008	0 ^h 38 ^m 14 ^s 29	-73°22'57".8	0.48587	2450625.81488	19.023	0.401
80337	0 ^h 38 ^m 36 ^s 33	-73°15'26".8	0.63648	2450625.74784	19.131	0.443
80394	0 ^h 38 ^m 38 ^s 05	-73°14'53".6	0.41094	2450625.60385	18.799	0.469
92549	0 ^h 39 ^m 09 ^s 14	-73°49'21".4	0.56439	2450625.82400	18.519	0.430
94151	0 ^h 39 ^m 20 ^s 43	-73°45'40".7	0.60091	2450625.31475	18.865	0.512
94527	0 ^h 38 ^m 41 ^s 20	-73°44'22".9	0.41058	2450625.50393	19.320	0.431
97728	0 ^h 38 ^m 47 ^s 38	-73°37'15".9	0.69867	2450625.90506	18.850	0.561
106157	0 ^h 38 ^m 51 ^s 91	-73°25'30".1	0.59299	2450625.83615	18.935	0.476
111096	0 ^h 39 ^m 15 ^s 77	-73°15'55".1	0.51772	2450625.62989	18.966	0.399
117869	0 ^h 39 ^m 01 ^s 05	-73°07'51".1	0.39714	2450625.90172	19.013	0.568

T a b l e 1
continued

SMC_SC2 No	α_{2000}	δ_{2000}	P [days]	T_0 [HJD]	$\langle I_0 \rangle$ [mag]	$\langle (V - I)_0 \rangle$ [mag]
4986	0 ^h 39 ^m 51 ^s .38	-73°33'07"7	0.52040	2450626.59921	19.006	0.338
7934	0 ^h 39 ^m 50 ^s .33	-73°26'27"0	0.63559	2450626.82501	18.913	0.516
9909	0 ^h 39 ^m 53 ^s .94	-73°22'46"5	0.60502	2450626.55993	18.836	0.431
14966	0 ^h 39 ^m 43 ^s .19	-73°12'45"8	0.59414	2450626.89838	18.691	0.344
20615	0 ^h 39 ^m 22 ^s .76	-72°59'50"6	0.54475	2450631.76348	19.073	0.492
21915	0 ^h 39 ^m 52 ^s .23	-72°59'01"7	0.59105	2450626.85530	18.917	0.467
22102	0 ^h 39 ^m 47 ^s .06	-72°57'00"0	0.55500	2450626.79323	18.884	0.375
38700	0 ^h 40 ^m 10 ^s .04	-73°20'44"6	0.58377	2450626.65693	19.235	0.542
38778	0 ^h 40 ^m 27 ^s .62	-73°19'54"9	0.59538	2450626.58459	19.342	0.432
40666	0 ^h 40 ^m 25 ^s .50	-73°14'52"6	0.60574	2450625.65070	19.067	0.491
40733	0 ^h 40 ^m 51 ^s .20	-73°14'17"8	0.60141	2450625.74524	18.923	0.434
60694	0 ^h 41 ^m 38 ^s .10	-73°25'40"5	0.55521	2450625.51823	19.119	0.401
62768	0 ^h 41 ^m 29 ^s .38	-73°22'02"3	0.62996	2450625.53537	19.031	0.558
66793	0 ^h 41 ^m 08 ^s .07	-73°16'18"5	0.59302	2450625.50098	19.540	0.094
68451	0 ^h 41 ^m 31 ^s .78	-73°13'28"6	0.60490	2450625.74907	18.772	0.575
71840	0 ^h 41 ^m 26 ^s .83	-73°03'55"2	0.70512	2450625.58965	18.744	0.579
78620	0 ^h 41 ^m 05 ^s .75	-72°52'38"2	0.53968	2450626.72688	18.765	0.390
79950	0 ^h 42 ^m 31 ^s .36	-73°42'27"2	0.55109	2450627.50791	18.923	0.492
87389	0 ^h 41 ^m 56 ^s .68	-73°28'31"6	0.56846	2450625.85428	18.671	0.484
88765	0 ^h 41 ^m 43 ^s .00	-73°25'53"5	0.57031	2450625.75882	18.790	0.394
93288	0 ^h 42 ^m 02 ^s .17	-73°17'58"8	0.57281	2450625.64184	18.856	0.453
95778	0 ^h 42 ^m 14 ^s .47	-73°16'44"7	0.37932	2450625.69130	18.755	0.374
101846	0 ^h 41 ^m 54 ^s .36	-73°05'39"3	0.52456	2450625.40453	19.116	0.391
102074	0 ^h 42 ^m 25 ^s .28	-73°03'49"8	0.70019	2450625.37980	18.544	0.513
102561	0 ^h 42 ^m 11 ^s .69	-73°03'29"3	0.63219	2450625.73632	19.147	0.612
104227	0 ^h 41 ^m 50 ^s .77	-73°02'20"5	0.57860	2450625.88320	19.037	0.559
105930	0 ^h 42 ^m 06 ^s .40	-72°59'49"0	0.60806	2450625.50982	19.025	0.570

T a b l e 1
continued

SMC_SC10 No	α_{2000}	δ_{2000}	P [days]	T_0 [HJD]	$\langle I_0 \rangle$ [mag]	$\langle (V - I)_0 \rangle$ [mag]
569	1 ^h 03 ^m 43 ^s .95	-72° 51' 26".3	0.63303	2450627.58372	18.835	0.426
742	1 ^h 03 ^m 38 ^s .66	-72° 49' 49".6	0.55599	2450627.61583	18.638	0.399
27643	1 ^h 03 ^m 26 ^s .63	-72° 14' 09".8	0.55935	2450633.72041	19.144	0.509
31598	1 ^h 03 ^m 32 ^s .65	-72° 09' 44".8	0.61412	2450627.85772	18.505	0.342
34580	1 ^h 03 ^m 24 ^s .10	-72° 05' 45".7	0.63711	2450649.62539	18.992	0.619
34778	1 ^h 03 ^m 44 ^s .21	-72° 04' 07".9	0.63294	2450627.40971	18.785	0.496
40178	1 ^h 04 ^m 03 ^s .48	-71° 57' 21".7	0.61683	2450627.60456	19.143	0.565
40184	1 ^h 03 ^m 59 ^s .89	-71° 57' 20".0	0.61190	2450627.54280	18.413	0.436
42272	1 ^h 04 ^m 32 ^s .12	-72° 49' 58".5	0.63000	2450627.68485	18.594	0.278
42305	1 ^h 04 ^m 48 ^s .81	-72° 49' 45".3	0.65008	2450627.37324	18.911	0.480
44989	1 ^h 04 ^m 09 ^s .83	-72° 46' 12".0	0.64449	2450627.37984	18.753	0.592
45509	1 ^h 04 ^m 42 ^s .63	-72° 46' 27".5	0.61453	2450627.67639	19.001	0.473
48245	1 ^h 04 ^m 46 ^s .16	-72° 42' 32".0	0.57381	2450627.77835	19.163	0.277
53289	1 ^h 04 ^m 03 ^s .41	-72° 35' 57".5	0.58480	2450627.57103	19.136	0.474
55506	1 ^h 04 ^m 46 ^s .98	-72° 34' 56".8	0.50373	2450627.59871	19.133	0.460
58154	1 ^h 04 ^m 48 ^s .36	-72° 29' 12".1	0.57906	2450627.82804	19.121	0.522
59960	1 ^h 04 ^m 15 ^s .01	-72° 24' 58".6	0.65442	2450627.74722	18.633	0.494
62320	1 ^h 04 ^m 27 ^s .10	-72° 23' 20".0	0.56045	2450627.77371	19.086	0.437
62519	1 ^h 04 ^m 31 ^s .16	-72° 21' 25".8	0.53328	2450627.70968	19.090	0.410
66339	1 ^h 04 ^m 34 ^s .90	-72° 17' 22".2	0.57881	2450627.69438	19.246	0.571
73049	1 ^h 04 ^m 46 ^s .98	-72° 06' 20".4	0.74960	2450627.23392	18.888	0.534
75595	1 ^h 04 ^m 11 ^s .34	-72° 01' 51".9	0.57364	2450627.46002	19.347	0.538
79096	1 ^h 05 ^m 03 ^s .64	-72° 51' 30".2	0.63683	2450627.87339	18.798	0.565
79441	1 ^h 04 ^m 55 ^s .17	-72° 51' 56".1	0.54148	2450627.63449	19.024	0.767
79766	1 ^h 05 ^m 01 ^s .93	-72° 49' 32".8	0.49610	2450627.56333	19.111	0.428
81646	1 ^h 04 ^m 50 ^s .99	-72° 47' 00".3	0.48898	2450627.46375	19.082	0.441
88729	1 ^h 05 ^m 23 ^s .14	-72° 38' 29".2	0.53593	2450627.70169	19.438	0.500
95100	1 ^h 05 ^m 15 ^s .11	-72° 25' 28".3	0.55114	2450627.76284	18.899	0.530
95483	1 ^h 05 ^m 16 ^s .55	-72° 25' 26".5	0.45596	2450627.80982	19.335	0.549
106764	1 ^h 05 ^m 35 ^s .89	-72° 06' 21".6	0.45383	2450627.78263	19.334	0.400
108491	1 ^h 05 ^m 09 ^s .24	-72° 02' 18".0	0.59966	2450627.35658	18.803	0.510
108725	1 ^h 04 ^m 55 ^s .88	-72° 03' 20".2	0.64366	2450627.49253	18.755	0.486
117057	1 ^h 05 ^m 53 ^s .86	-72° 44' 36".4	0.59789	2450627.74985	18.836	0.565
141261	1 ^h 06 ^m 11 ^s .30	-71° 57' 32".7	0.64287	2450627.66534	18.798	0.540

T a b l e 1
concluded

SMC_SC11 No	α_{2000}	δ_{2000}	P [days]	T_0 [HJD]	$\langle I_0 \rangle$ [mag]	$\langle (V - I)_0 \rangle$ [mag]
5571	1 ^h 06 ^m 40 ^s .65	-72°56'37".3	0.57429	2450625.48276	18.934	0.530
5854	1 ^h 06 ^m 53 ^s .16	-72°54'06".9	0.56249	2450625.72605	18.946	0.403
13987	1 ^h 06 ^m 54 ^s .39	-72°41'45".6	0.57828	2450625.75546	18.938	0.502
17783	1 ^h 06 ^m 48 ^s .19	-72°35'53".4	0.52500	2450625.54465	19.134	0.540
17796	1 ^h 06 ^m 33 ^s .08	-72°35'44".9	0.62707	2450625.72529	19.092	0.590
22629	1 ^h 06 ^m 55 ^s .61	-72°27'54".5	0.51038	2450625.66882	18.918	0.332
35737	1 ^h 07 ^m 25 ^s .94	-72°59'41".5	0.58074	2450625.50963	18.747	0.593
43077	1 ^h 07 ^m 28 ^s .51	-72°45'27".5	0.57957	2450625.59858	19.393	0.426
51341	1 ^h 07 ^m 28 ^s .57	-72°30'52".9	0.57539	2450625.83346	18.823	0.493
55977	1 ^h 07 ^m 42 ^s .39	-72°23'52".8	0.52993	2450625.58127	18.775	0.409
58352	1 ^h 07 ^m 21 ^s .86	-72°18'25".9	0.67319	2450625.79673	18.755	0.592
61762	1 ^h 07 ^m 34 ^s .50	-72°14'29".8	0.64675	2450625.77628	18.846	0.508
81273	1 ^h 08 ^m 04 ^s .44	-72°33'49".4	0.64620	2450625.34023	18.727	0.559
87493	1 ^h 08 ^m 18 ^s .40	-72°23'15".4	0.56204	2450625.85829	19.024	0.471
92360	1 ^h 08 ^m 02 ^s .60	-72°16'00".8	0.62923	2450625.72205	18.666	0.521
95929	1 ^h 08 ^m 47 ^s .55	-73°05'21".1	0.56806	2450625.66490	19.153	0.544
96926	1 ^h 08 ^m 42 ^s .27	-73°04'11".2	0.75503	2450625.61762	18.789	0.552
98254	1 ^h 08 ^m 34 ^s .93	-73°00'05".6	0.55730	2450625.60369	18.933	0.478
101421	1 ^h 08 ^m 36 ^s .97	-72°53'21".6	0.61936	2450625.37421	18.977	0.523
103038	1 ^h 09 ^m 09 ^s .89	-72°46'46".4	0.65870	2450627.87426	18.773	0.538
106152	1 ^h 09 ^m 09 ^s .67	-72°41'49".8	0.56562	2450627.85579	18.720	0.559
110962	1 ^h 08 ^m 46 ^s .40	-72°32'43".2	0.57974	2450625.45702	19.013	0.446
114006	1 ^h 08 ^m 38 ^s .76	-72°27'57".9	0.62280	2450625.73419	18.692	0.379
115856	1 ^h 08 ^m 48 ^s .74	-72°23'42".8	0.62708	2450625.59297	18.899	0.505
120659	1 ^h 08 ^m 38 ^s .27	-72°13'33".3	0.57832	2450625.36682	18.906	0.491

Table 2
RR Lyrae in the LMC fields

LMC_SC14 No	α_{2000}	δ_{2000}	P [days]	T_0 [HJD]	$\langle I_0 \rangle$ [mag]	$\langle (V - I)_0 \rangle$ [mag]
56486	5 ^h 02 ^m 30 ^s 87	-68°47'27".5	0.50450	2450726.60063	18.370	-
60196	5 ^h 02 ^m 54 ^s 80	-68°46'06".6	0.53955	2450726.52917	18.433	0.373
60396	5 ^h 02 ^m 30 ^s 19	-68°44'48".0	0.37880	2450726.78513	18.325	0.541
60440	5 ^h 03 ^m 01 ^s 47	-68°44'32".6	0.60690	2450726.67184	18.430	0.537
60491	5 ^h 02 ^m 51 ^s 09	-68°44'02".2	0.74636	2450726.51712	18.125	0.564
67299	5 ^h 02 ^m 58 ^s 49	-68°38'30".0	0.56493	2450726.54835	18.494	0.273
116685	5 ^h 03 ^m 11 ^s 18	-68°54'37".5	0.59493	2450726.44067	18.361	0.364
121101	5 ^h 03 ^m 32 ^s 21	-68°53'02".4	0.64537	2450726.17221	18.438	0.440
121657	5 ^h 03 ^m 39 ^s 96	-68°53'44".1	0.43272	2450726.38449	18.461	0.314
125651	5 ^h 03 ^m 30 ^s 10	-68°49'36".2	0.64286	2450726.22417	18.351	0.404
125838	5 ^h 03 ^m 37 ^s 69	-68°48'22".9	0.58212	2450726.34026	18.362	0.424
133251	5 ^h 03 ^m 22 ^s 90	-68°43'02".2	0.49293	2450726.48555	18.405	0.224
133463	5 ^h 03 ^m 22 ^s 99	-68°41'39".9	0.67098	2450726.67914	18.321	0.286
136634	5 ^h 03 ^m 27 ^s 31	-68°39'04".1	0.60485	2450726.44668	18.570	0.582
136961	5 ^h 03 ^m 14 ^s 49	-68°36'49".0	0.59008	2450726.30085	18.616	0.515
137336	5 ^h 03 ^m 45 ^s 19	-68°38'21".6	0.50530	2450726.50278	18.554	0.406
137475	5 ^h 03 ^m 33 ^s 73	-68°37'34".9	0.57833	2450726.26638	18.632	0.476
188216	5 ^h 04 ^m 04 ^s 00	-68°54'12".7	0.49736	2450726.51500	18.423	0.535
192784	5 ^h 03 ^m 53 ^s 68	-68°52'45".2	0.59022	2450726.79298	18.508	0.461
193081	5 ^h 03 ^m 53 ^s 28	-68°51'01".9	0.50587	2450726.63093	18.451	0.352
196815	5 ^h 04 ^m 02 ^s 49	-68°49'55".9	0.55193	2450726.42734	18.516	0.373
197090	5 ^h 03 ^m 48 ^s 13	-68°48'31".9	0.80632	2450726.67050	18.264	0.486
197167	5 ^h 04 ^m 25 ^s 46	-68°48'04".4	0.60230	2450726.24401	18.459	0.646
201276	5 ^h 03 ^m 52 ^s 00	-68°45'44".4	0.61590	2450726.74991	18.170	0.264
201334	5 ^h 03 ^m 54 ^s 65	-68°45'23".1	0.67399	2450726.58759	18.213	0.336
205106	5 ^h 04 ^m 08 ^s 32	-68°42'52".1	0.46069	2450726.44708	18.103	0.260
206307	5 ^h 04 ^m 14 ^s 80	-68°40'08".8	0.56461	2450726.61964	18.353	0.463
208439	5 ^h 04 ^m 13 ^s 09	-68°37'42".2	0.58141	2450726.65596	18.439	0.406
208851	5 ^h 04 ^m 06 ^s 59	-68°36'57".3	0.46795	2450726.60989	18.423	0.437
263312	5 ^h 04 ^m 45 ^s 57	-68°54'21".3	0.49424	2450726.35373	18.696	0.488
271214	5 ^h 04 ^m 35 ^s 05	-68°50'05".9	0.62875	2450726.76635	18.129	0.362
271741	5 ^h 05 ^m 03 ^s 12	-68°47'21".7	0.58289	2450726.22424	18.170	0.448
271809	5 ^h 04 ^m 34 ^s 12	-68°47'01".9	0.60660	2450726.23272	18.274	0.340
272336	5 ^h 04 ^m 57 ^s 71	-68°48'34".8	0.47570	2450726.61568	18.843	0.470
276073	5 ^h 04 ^m 30 ^s 65	-68°44'40".5	0.76915	2450726.79519	18.096	0.341
277030	5 ^h 04 ^m 45 ^s 92	-68°44'29".2	0.54504	2450726.28436	18.565	0.384
280488	5 ^h 04 ^m 47 ^s 68	-68°42'02".7	0.59182	2450726.45974	18.359	0.430
280833	5 ^h 04 ^m 34 ^s 35	-68°40'12".7	0.53919	2450726.50994	18.420	0.329
281168	5 ^h 04 ^m 59 ^s 00	-68°42'24".4	0.49011	2450726.43397	18.562	0.546
284645	5 ^h 04 ^m 49 ^s 22	-68°39'10".9	0.60222	2450726.73851	18.246	0.406
285135	5 ^h 04 ^m 38 ^s 26	-68°39'30".9	0.50788	2450726.48244	18.349	0.384
285608	5 ^h 04 ^m 46 ^s 19	-68°37'24".5	0.62395	2450726.69614	18.287	0.397

Table 2

continued

LMC_SC15 No	α_{2000}	δ_{2000}	P [days]	T_0 [HJD]	$\langle I_0 \rangle$ [mag]	$\langle (V - I)_0 \rangle$ [mag]
42752	5 ^h 00 ^m 16 ^s .89	-68°50'03".2	0.57959	2450726.56009	18.320	0.400
43098	5 ^h 00 ^m 35 ^s .72	-68°47'40".1	0.59998	2450726.53192	18.258	0.249
50667	5 ^h 00 ^m 20 ^s .51	-68°40'21".8	0.46970	2450726.77800	18.540	0.481
53231	5 ^h 00 ^m 37 ^s .29	-68°38'47".7	0.57335	2450726.48830	18.452	0.440
53354	5 ^h 00 ^m 17 ^s .39	-68°37'46".7	0.61109	2450726.37879	18.344	0.574
93940	5 ^h 01 ^m 13 ^s .42	-68°55'11".1	0.56620	2450726.49747	18.568	0.479
96987	5 ^h 01 ^m 14 ^s .54	-68°52'59".2	0.65320	2450726.41143	18.674	0.528
97214	5 ^h 00 ^m 59 ^s .55	-68°51'52".4	0.58351	2450726.45683	18.401	0.395
97443	5 ^h 01 ^m 03 ^s .25	-68°50'42".6	0.54864	2450726.42722	18.382	0.516
99815	5 ^h 00 ^m 47 ^s .38	-68°49'30".2	0.64957	2450726.18178	18.315	0.510
103919	5 ^h 01 ^m 11 ^s .51	-68°45'02".3	0.57616	2450726.38472	18.433	0.467
106588	5 ^h 01 ^m 13 ^s .06	-68°42'30".3	0.55930	2450726.69822	18.518	0.391
106642	5 ^h 01 ^m 10 ^s .05	-68°41'58".9	0.53240	2450726.56595	18.649	0.483
110089	5 ^h 00 ^m 45 ^s .15	-68°39'46".0	0.51924	2450726.78655	18.706	0.508
153469	5 ^h 01 ^m 38 ^s .80	-68°52'58".0	0.52058	2450726.75941	18.384	-
153750	5 ^h 01 ^m 21 ^s .50	-68°51'30".9	0.49378	2450726.59390	18.675	0.617
162619	5 ^h 01 ^m 53 ^s .00	-68°40'14".6	0.53499	2450726.56687	18.379	0.545
165683	5 ^h 01 ^m 39 ^s .02	-68°36'32".9	0.53603	2450726.32196	18.369	-
208481	5 ^h 02 ^m 26 ^s .61	-68°53'01".4	0.69586	2450726.37393	18.165	0.465
208661	5 ^h 02 ^m 19 ^s .09	-68°51'55".5	0.58506	2450726.64076	18.221	0.440
208809	5 ^h 02 ^m 10 ^s .19	-68°50'56".4	0.33933	2450726.77710	18.173	0.412
209402	5 ^h 02 ^m 17 ^s .47	-68°51'24".5	0.69433	2450726.18327	18.294	-
212860	5 ^h 02 ^m 30 ^s .87	-68°47'27".5	0.50439	2450726.72583	18.344	0.288
215146	5 ^h 02 ^m 18 ^s .26	-68°46'11".4	0.51185	2450726.75625	18.216	0.300
215934	5 ^h 02 ^m 30 ^s .21	-68°44'48".1	0.61067	2450726.57878	18.349	0.547

Table 2
continued

LMC_SC19 No	α_{2000}	δ_{2000}	P [days]	T_0 [HJD]	$\langle I_0 \rangle$ [mag]	$\langle (V - I)_0 \rangle$ [mag]
6663	5 ^h 42 ^m 24 ^s .74	-70°55'23".0	0.74270	2450726.63713	18.160	0.422
6664	5 ^h 42 ^m 45 ^s .68	-70°55'22".8	0.61427	2450726.77286	18.287	0.559
7355	5 ^h 42 ^m 24 ^s .43	-70°54'09".5	0.49533	2450726.45278	18.623	0.567
52480	5 ^h 43 ^m 03 ^s .78	-71°02'16".5	0.62276	2450726.62549	18.324	0.496
52569	5 ^h 43 ^m 37 ^s .50	-71°01'34".8	0.56999	2450726.31477	18.636	0.572
55410	5 ^h 43 ^m 05 ^s .25	-70°58'38".5	0.71703	2450726.14388	18.434	0.496
58286	5 ^h 43 ^m 35 ^s .03	-70°55'49".2	0.70344	2450726.20714	18.341	0.391
58628	5 ^h 43 ^m 35 ^s .32	-70°53'33".3	0.58370	2450726.71057	18.509	0.451
58871	5 ^h 43 ^m 24 ^s .59	-70°55'40".2	0.56959	2450726.68139	18.590	0.550
58898	5 ^h 43 ^m 43 ^s .08	-70°55'27".7	0.57292	2450726.39797	18.450	0.461
106413	5 ^h 44 ^m 01 ^s .96	-70°58'09".2	0.60761	2450726.39086	18.709	0.670
108632	5 ^h 44 ^m 06 ^s .20	-70°55'26".3	0.53913	2450726.78619	18.276	0.327
109458	5 ^h 44 ^m 06 ^s .92	-70°53'07".4	0.54682	2450726.44028	18.593	0.436
114824	5 ^h 43 ^m 57 ^s .14	-70°47'26".5	0.52157	2450726.66141	18.745	0.547
114971	5 ^h 43 ^m 49 ^s .78	-70°46'21".7	0.55346	2450726.38831	18.436	0.349
114999	5 ^h 44 ^m 03 ^s .12	-70°46'07".4	0.61682	2450726.44564	18.330	0.424
117483	5 ^h 44 ^m 24 ^s .33	-70°45'08".0	0.54334	2450726.64716	18.728	0.508
152545	5 ^h 45 ^m 03 ^s .23	-70°56'13".6	0.58623	2450726.60329	18.262	0.430
153061	5 ^h 44 ^m 45 ^s .04	-70°56'50".3	0.57814	2450726.45170	18.420	0.442
155215	5 ^h 44 ^m 58 ^s .58	-70°55'29".3	0.61142	2450726.79582	18.598	0.508
155332	5 ^h 44 ^m 31 ^s .83	-70°54'38".0	0.53793	2450726.42698	18.513	0.420
156126	5 ^h 44 ^m 44 ^s .35	-70°53'01".7	0.56410	2450726.35580	18.679	0.612
161047	5 ^h 45 ^m 09 ^s .98	-70°48'29".2	0.85804	2450726.60803	17.956	0.566
161929	5 ^h 45 ^m 10 ^s .19	-70°46'17".7	0.64948	2450726.57704	18.400	0.671

T a b l e 2
concluded

LMC_SC20 No	α_{2000}	δ_{2000}	P [days]	T_0 [HJD]	$\langle I_0 \rangle$ [mag]	$\langle (V - I)_0 \rangle$ [mag]
4046	5 ^h 44 ^m 52 ^s .71	-71°06'46"5	0.51414	2450726.58837	18.446	-
7253	5 ^h 45 ^m 11 ^s .20	-71°05'14"4	0.51568	2450726.63141	18.346	0.370
7267	5 ^h 45 ^m 19 ^s .08	-71°05'07"8	0.58154	2450726.69251	18.331	0.406
7434	5 ^h 45 ^m 12 ^s .18	-71°03'41"8	0.48940	2450726.74994	18.695	0.378
10801	5 ^h 45 ^m 22 ^s .70	-71°01'43"1	0.58318	2450726.51069	18.606	0.584
14634	5 ^h 45 ^m 03 ^s .25	-70°56'13"6	0.58607	2450726.78854	18.252	0.375
14699	5 ^h 45 ^m 14 ^s .61	-70°55'52"7	0.69457	2450726.64720	18.256	0.414
14753	5 ^h 44 ^m 58 ^s .59	-70°55'29"2	0.37935	2450726.58181	18.561	0.637
57576	5 ^h 46 ^m 00 ^s .10	-71°11'55"3	0.57116	2450726.76965	18.301	0.376
61466	5 ^h 46 ^m 04 ^s .14	-71°06'21"3	0.48264	2450726.52647	18.767	0.392
63901	5 ^h 45 ^m 37 ^s .66	-71°03'56"6	0.59741	2450726.33563	18.296	0.577
73467	5 ^h 45 ^m 55 ^s .95	-70°55'05"7	0.52878	2450726.51206	18.476	0.488
110873	5 ^h 46 ^m 31 ^s .67	-71°11'08"0	0.40794	2450726.81053	18.672	0.835
115941	5 ^h 46 ^m 34 ^s .32	-71°05'13"6	0.59333	2450726.69932	18.475	0.251
121823	5 ^h 46 ^m 47 ^s .10	-70°58'23"5	0.69004	2450726.76861	18.119	0.415
122510	5 ^h 46 ^m 29 ^s .15	-70°57'14"0	0.34967	2450726.57619	18.899	0.409
122544	5 ^h 46 ^m 37 ^s .42	-70°57'01"6	0.60147	2450726.81148	18.467	0.491
160617	5 ^h 47 ^m 22 ^s .69	-71°10'21"4	0.53690	2450726.71620	18.461	0.450
160691	5 ^h 47 ^m 13 ^s .65	-71°09'43"7	0.54662	2450726.47920	18.374	0.452

Table 3
RR Lyrae in the Baade's Window

Bulge No	P [days]	T_0 [HJD]	$\langle I_0 \rangle$ [mag]	$\langle (V - I)_0 \rangle$ [mag]
BWC_V6	0.42765	2448724.80690	14.280	0.746
BWC_V14	0.44022	2448724.38420	14.851	0.412
BWC_V15	0.45871	2448724.48660	14.770	0.445
BWC_V22	0.48968	2448724.33960	14.765	0.534
BWC_V23	0.45426	2448724.85360	14.975	0.499
BWC_V26	0.47863	2448724.53570	14.982	0.709
BWC_V28	0.59478	2448724.10300	14.676	0.651
BWC_V30	0.57147	2448724.48110	14.710	0.589
BWC_V33	0.55032	2448724.54030	14.993	0.716
BWC_V41	0.46214	2448724.44140	14.969	0.713
BWC_V51	0.64949	2448724.51580	14.935	0.742
BWC_V56	0.68046	2448724.33270	14.700	0.788
BWC_V61	0.61595	2448724.38800	14.887	0.734
BW1_V10	0.55564	2448724.23230	14.511	0.553
BW1_V14	0.49322	2448724.45880	14.748	0.694
BW1_V18	0.52956	2448724.59160	14.793	0.519
BW1_V19	0.44444	2448724.46390	14.856	0.638
BW1_V21	0.45411	2448724.46440	14.855	0.632
BW1_V25	0.60023	2448724.05450	14.754	0.661
BW1_V34	0.63271	2448724.42450	15.005	0.685
BW1_V36	0.44856	2448724.47150	15.096	0.654
BW1_V40	0.61175	2448724.54750	14.917	0.718
BW1_V43	0.42178	2448724.59700	15.370	0.525
BW2_V23	0.49276	2448724.79820	15.228	0.360
BW2_V24	0.59743	2448724.36300	14.747	0.747
BW3_V11	0.65494	2448724.19990	14.077	0.558
BW3_V13	0.45751	2448724.38470	14.762	0.622
BW3_V16	0.60354	2448724.27520	14.441	0.601
BW3_V17	0.40333	2448724.41900	15.016	0.498
BW3_V21	0.77304	2448723.87470	14.656	0.669
BW3_V43	0.64089	2448724.84020	14.674	0.702
BW3_V46	0.48653	2448724.87620	15.045	0.577
BW3_V61	0.54160	2448724.52000	15.648	0.637
BW3_V99	0.56046	2448724.29930	15.484	0.512
BW4_V5	0.47468	2448724.66310	14.476	0.661
BW4_V8	0.51586	2448724.50730	14.581	0.620
BW4_V9	0.46317	2448724.76840	14.650	0.610
BW4_V11	0.60169	2448723.88420	14.455	0.598
BW4_V12	0.63958	2448724.38510	14.452	0.704
BW4_V22	0.56093	2448724.64860	14.828	0.788
BW4_V43	0.55992	2448724.40770	15.126	0.642

T a b l e 3
concluded

Bulge No	P [days]	T_0 [HJD]	$\langle I_0 \rangle$ [mag]	$\langle (V - I)_0 \rangle$ [mag]
BW5_V13	0.49492	2448724.11000	14.856	0.490
BW5_V24	0.55213	2448724.47350	14.841	0.539
BW5_V28	0.46723	2448724.35270	15.097	0.547
BW5_V29	0.47361	2448724.41920	14.917	0.450
BW5_V34	0.49027	2448724.42790	15.056	0.696
BW5_V36	0.59451	2448724.39800	14.850	0.811
BW5_V39	0.50786	2448724.29470	15.217	0.822
BW5_V50	0.49635	2448724.35630	15.439	0.525
BW6_V7	0.52501	2448724.43400	14.444	0.524
BW6_V12	0.55603	2448724.06230	14.626	0.681
BW6_V15	0.55745	2448724.68390	14.542	1.067
BW6_V17	0.65163	2448724.17530	14.603	0.727
BW6_V18	0.54140	2448724.54480	14.806	0.750
BW6_V20	0.39370	2448724.62220	14.972	0.650
BW6_V27	0.58400	2448724.21080	14.660	0.827
BW6_V35	0.43124	2448724.70570	15.161	0.713
BW7_V8	0.50711	2448724.64700	14.319	0.497
BW7_V15	0.49708	2448724.33310	14.772	0.585
BW7_V18	0.66695	2448724.95130	14.342	0.570
BW7_V20	0.77051	2448724.27480	14.564	0.663
BW7_V23	0.60579	2448724.19770	14.555	0.711
BW7_V25	0.52116	2448724.51250	14.827	0.636
BW7_V33	0.51122	2448724.78270	14.861	0.772
BW7_V48	0.63862	2448724.27360	15.380	0.647
BW8_V7	0.55454	2448724.25970	14.325	0.575
BW8_V8	0.78117	2448724.86720	14.221	0.617
BW8_V15	0.57724	2448724.14010	14.646	0.585
BW8_V16	0.42413	2448724.67060	14.809	0.554
BW8_V18	0.70001	2448724.09170	14.441	0.649
BW8_V20	0.67699	2448724.23240	14.538	0.625
BW8_V26	0.61699	2448724.90460	14.651	0.666
BW8_V35	0.64770	2448724.17200	14.755	0.723